

The Magic 4-Cyanoresocinols - Their Role in the Understanding of Phenomena at the Rod-Banana Cross-Over and Relations to Twist-Bend Phases and Other Newly Emerging LC Phase Types

Carsten Tschierske

To cite this article: Carsten Tschierske (2022): The Magic 4-Cyanoresocinols - Their Role in the Understanding of Phenomena at the Rod-Banana Cross-Over and Relations to Twist-Bend Phases and Other Newly Emerging LC Phase Types, Liquid Crystals, DOI: [10.1080/02678292.2021.2010142](https://doi.org/10.1080/02678292.2021.2010142)

To link to this article: <https://doi.org/10.1080/02678292.2021.2010142>



© 2022 The Author(s). Published by Informa UK Limited, trading as Taylor & Francis Group.



[View supplementary material](#)



Published online: 27 Jan 2022.



[Submit your article to this journal](#)



Article views: 409



[View related articles](#)



[View Crossmark data](#)

The Magic 4-Cyanoresocinols - Their Role in the Understanding of Phenomena at the Rod-Banana Cross-Over and Relations to Twist-Bend Phases and Other Newly Emerging LC Phase Types

Carsten Tschierske

Institute of Chemistry, Organic Chemistry, Martin Luther University Halle-Wittenberg, Halle, Germany

ABSTRACT

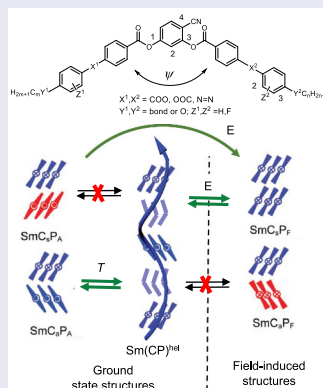
In this account, bent-core molecules involving the polar cyano-group are reviewed with a focus on the intensely investigated class of 4-cyanoresorcinol bisbenzoates. Cybotaxis and phase biaxiality of their nematic phases, the transition from nematic to smectic phases and the development of tilt and polar order in their smectic phases are discussed. Of special interest are heliconical (twist-bend) smectic intermediate phases occurring at the transition from paraelectric to antiferroelectric polar smectic phases if coinciding with the transition between anticlinic and synclinic tilt correlation. For some compounds, a reentrant polar SmA phase ($\text{SmA}^{\text{LT}}\text{P}_F$) is observed below SmC and a silylated compound forms a new leaning-type phase. The formation of these achiral phases instead of the polar SmC phases involving layer chirality is discussed under the aspect of enantiophobic vs. enantiophilic organization. The effects of core structure and chain branching and, in addition, the effects of the intrinsic transient molecular, superstructural, and permanent molecular chirality on LC self-assembly are discussed.

ARTICLE HISTORY

Received 23 August 2021
Accepted 20 November 2021

KEYWORDS

Bent-core liquid crystals; paraelectric and ferroelectric liquid crystals; biaxiality; synclinic and anticlinic tilt correlation; mirror symmetry breaking; heliconical phases; twist-bend smectic phases; diastereomerism; chirality; 4-cyanoresorcinol; leaning phase; magnetic field effects




1. Preamble

Prof. B. K. Sadashiva is well known to me from his papers, several conferences and some visits at the Raman Research Institute (RRI) in Bangalore where he kindly invited and hosted me. Moreover, two of his former students Dr R. A. Reddy and Dr H. N. S. Murthy worked in Halle as Postdocs with me and Prof. Weissflog, respectively. Especially, I remember a post-conference excursion after the Keystone conference to Arches National Park with Prof. B. K. Sadashiva, Prof. W. Weissflog and Prof. R. Stannarius (Figure 1) where we got to know him more personally. Like me, BKS was a synthetic organic chemist focusing upon structure–property relationships

to find new properties and phases in liquid crystalline (LC) materials. Besides being well known for his co-authorship in the fundamental paper on discotic LCs together with S. Chandrasekhar and K. A. Suresh [1], he is also well recognized for his work on re-entrant nematic phases [2] and on metallomesogens [3,4], with a focus on the search for phase biaxiality. Since the beginning of this century his work was focused on bent-core liquid crystals (BCLCs), especially fluorine substituted [5,6,7] and those forming non-tilted biaxial and polar smectic phases, where he made significant contributions [8,9–11]. The research interests and topics of ours and B.K. Sadashivas were occasionally closely related, and in fact, the reports

CONTACT Carsten Tschierske  carsten.tschierske@chemie.uni-halle.de

 Supplemental data for this article can be accessed [here](#)

© 2022 The Author(s). Published by Informa UK Limited, trading as Taylor & Francis Group.

This is an Open Access article distributed under the terms of the Creative Commons Attribution-NonCommercial-NoDerivatives License (<http://creativecommons.org/licenses/by-nc-nd/4.0/>), which permits non-commercial re-use, distribution, and reproduction in any medium, provided the original work is properly cited, and is not altered, transformed, or built upon in any way.



Figure 1. Left side: Prof. R. Stannarius, Prof. W. Weissflog, Prof. B. K. Sadashiva, (left to right in the inset) and I (the photographer) hiking in the Arches National Park after the Keystone ILCC in 2006; right-hand side pictures were used with courtesy of W. Weissflog.

on ferroelectric switching in achiral bent-core LCs appeared almost simultaneously in the same year 2002 from both of our groups. We reported it for chain-silylated BCLCs [12], whereas his compounds were based on core-fluorinated BCLCs [13]. The same happened when the first SmA_b phases were found in low molecular weight systems. He and his colleagues from the Raman Research Institute (RRI) reported them for mixtures of rod-like and bent-core molecules [14], whereas our approach was based on sanidic metallomesogens [15].

BKS also provided first reports on BCLC involving cyano groups. After its introduction by G. Gray in 1973 [16], the CN group became one of the most influential groups in LC science. BKS has shown in his work that replacing one terminal alkyl chain at the bent core by a CN end group leads to antiparallel packing of the aromatic cores (CN3, CN4, Scheme 1, Figure 2). In these LC phases, the alkyl chain density is reduced so that the onset of polar order cannot induce interface curvature. As a consequence, flat layers can be retained and also the emergence of tilt can be avoided, leading to biaxial SmA phases showing paraelectric and antiferroelectric (AF) switching. Because in these SmA phases

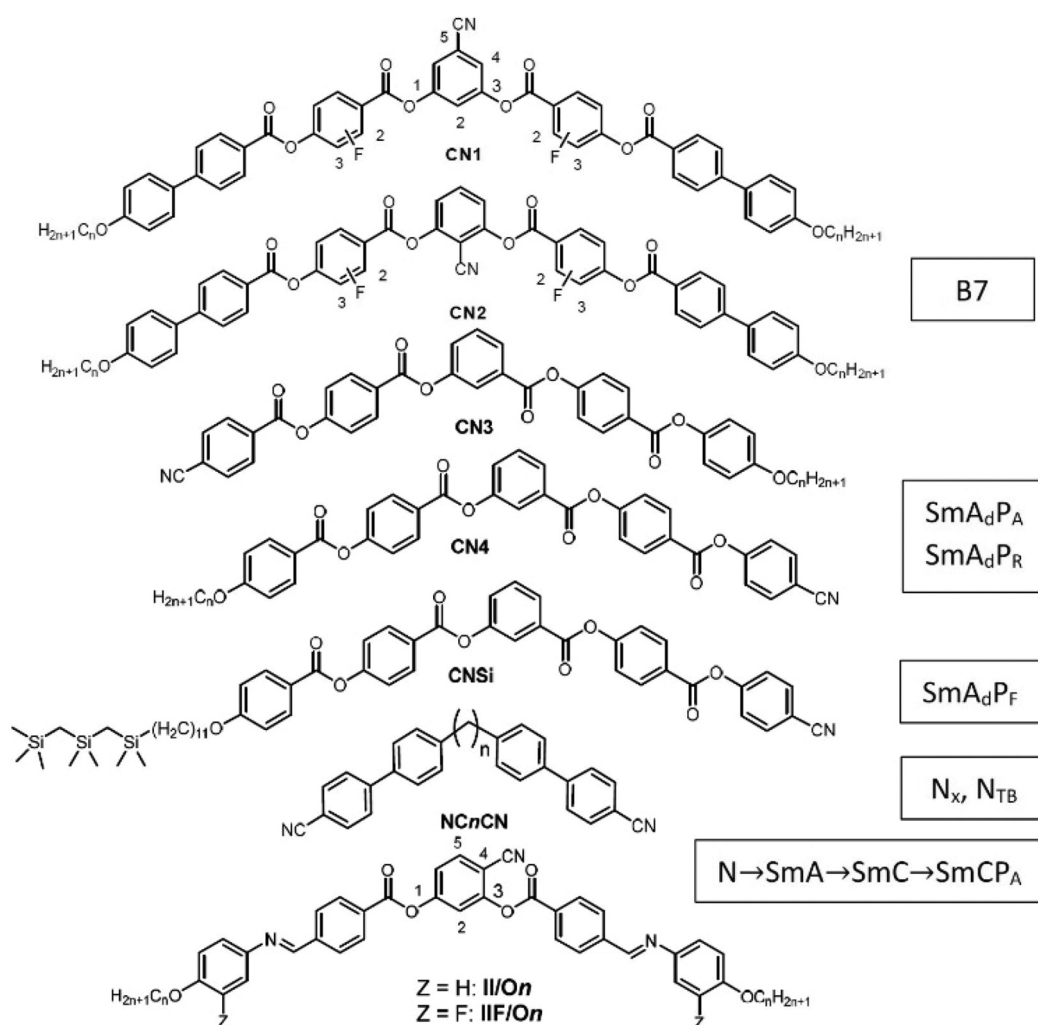
the layer distance is larger than the molecular length, they were notated as SmA_dP_A , SmA_dP_R , etc. phases (Figure 2) [10,17,18]. I had the pleasure to work together with one of his most talented students Dr. R. A. Reddy who was a postdoc at Halle University for several years. During that period, we produced a series of papers about silylated BCLCs [19,20,120], including a well cited review about BCLCs [22]. Later on, when he moved to Boulder, he combined the concept of polar end-groups, retaining non-tilted phases, with our concept of chain silylation to induce ferroelectricity in BCLCs [12,19,20,23], which then led to the first ferroelectric (FE) switching non-tilted SmA_dP_F phase (CNSi, Scheme 1) [24].

Later, bent molecules with CN groups at both ends (the bent dimesogens NCnCN in Scheme 1) lead to the first compounds showing the twist-bend nematic (N_x , N_{TB}) phase, theoretically predicted by R. B. Meyer [25] and I. Dozov [26] and experimentally observed by V.P. Panov et al. [27] and others [28–35].

During his research, BKS also introduced the CN group into other positions at the bent polyaromatic core. Thus, he reported first examples of BCLCs having CN groups attached to the central bent unit, either in 2- or in 5-position, (CN2 and CN1, Scheme 1) [36–38]. Similar to the related NO_2 substituted compounds, this polar substituent provides polar and modulated smectic phases (B7 phases) showing fascinating textures involving helical filaments [39,40]. The only remaining substitution pattern being unexplored at that time was the 4-CN substitution. This class of compounds was found to provide new phase structures and a variety of insights into the principles of development of chirality, polarity and tilt in soft self-assembly as will be shown in this review.

2. Introduction

4-Cyanoresorcinol based LCs (compounds **II/On**, **IIF/On**, **BB/On** and **TT/O8,O12**, Scheme 2) have been first synthesized and investigated by W. Weissflog et al. in Halle and lead to phase sequences like $\text{N} - \text{SmA} - \text{SmC} - \text{B2}$, on cooling [41,42,43], involving LC phases being typical for rod-like as well as for BCLCs [44,45,46]. The main focus of his work was on the Schiff base derived compounds **II/On** and **IIF/On** (Scheme 1). For a peripheral core-fluorinated compound of type **IIF/On**, a non-tilted single layer biaxial SmAP_A phase was for the first time postulated based on apparent X-ray evidence [46]. Further work was focused on the transition between the uniaxial and biaxial smectic phases in thin films [47] and in bulk [48]. NMR studies revealed an opening angle ψ between the two



Scheme 1. Examples of bent molecules involving CN substituted aromatic cores and their typical LC phases; compounds **CN1–CN4** have been reported by B.K. Sadashiva et al.

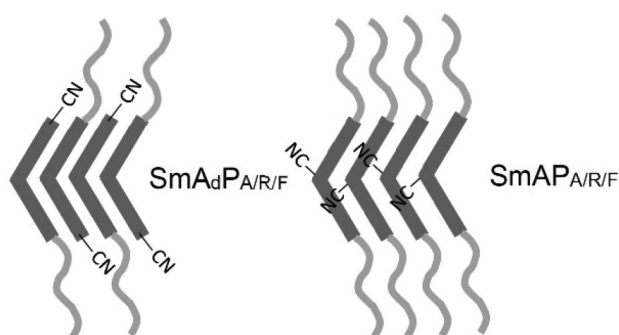
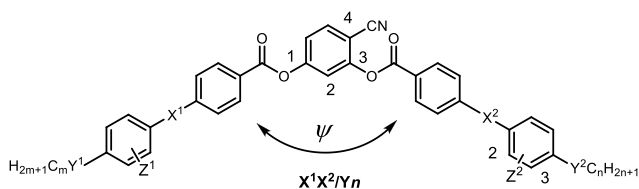


Figure 2. The intercalated double layer and ‘single layer’ polar SmA phases of BCLCs [A, R, and F stand for **antipolar**, **randomized** and **synpolar (ferroelectric)** order between adjacent layers].

Schiff base wings (Scheme 2) being substantially larger than 120° , increasing from 136° at 77°C to 143° at 167°C [121]. This widening of the opening angle is due to a combination

of dipole compensation between $\text{C}=\text{O}$ and CN , steric and stereoelectronic interactions around the COO group in 3-position, and it leads to molecules with an effective average shape at the cross-over between classical rod-like ($\psi = 180^\circ$) and bent-core mesogens ($\alpha\psi \sim 120^\circ$), showing transitions from non-polar to polar LC phases [44]. The large opening angle ψ of the core and the presence of the CN group also promote nematic phases [44,50], which are rare among the typical bent-core mesogens with 120° bend [22,51,52,53].

Our interest in these bent compounds arose from their capability of forming weakly tilted and orthogonal smectic as well as nematic phases. The initial target was to use them as building blocks for the design of LCs forming the orthorhombic biaxial nematic phase [53]. Though this phase was never achieved, the research on these compounds was very fruitful and led to new knowledges and LC phase types. The focus of this review is on the 4-cyanoresorcinol bisbenzoates collated in Scheme 2. Most of



Comp.	X ¹	X ²
II/Y_n	N=C	C=N
PP/Y_n	-	-
BB/Y_n	COO	OOC
TT/Y_n	OOC	COO
TB/Y_n	OOC	OOC
AA/Y_n	N=N	N=N
AB/Y_n	N=N	OOC
AT/Y_n	N=N	COO

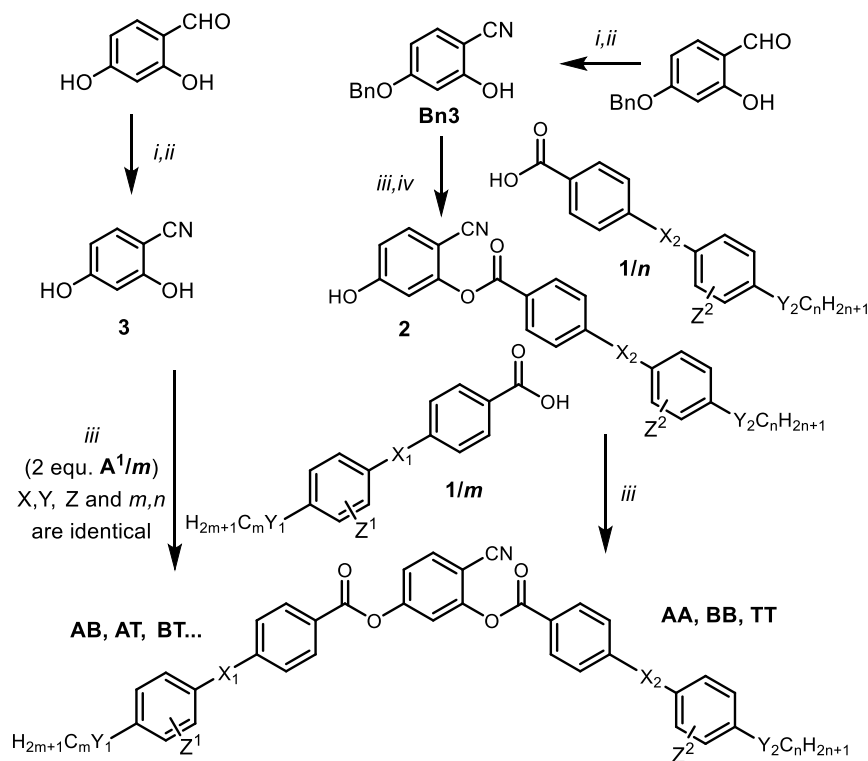
Scheme 2. Major compounds under discussion and the used abbreviations. The initial letters indicate the type of rod-like wing groups attached to the 4-cyanoresorcinol unit; **I** = imine (Schiff base), **B** = phenylbenzoate, **T** = phenylterephthalate, **A** = azobenzene and **P** = biphenyl; combinations indicate two different wing groups, the first letter indicating that one at the 1-position and the second that at the 3 position of the 4-cyanoresorcinol core unit. The connecting unit Y (single bond or O) and chain length m , n is given after the slash, only one number n indicates two identical chains ($m = n$). For compounds being fluorinated at the outer ring ($Z = F$) **F** is added before the slash.

these compounds involve COO groups with different directions and in some cases also azo groups (N=N) as linking units X in their rod-like wings. Compounds with identical wings (**AA**, **BB**, **PP**, **TT**) as well as those combining different wings (**BT**, **TB**, **AB**, **AT** . . .) and compounds being fluorinated at the periphery ($Z = F$) or having branched chains were also investigated. These investigations have been spread over numerous scientific papers and the models proposed for their organization have changed during the course of the ongoing investigations. The purpose of this contribution is to summarize the major conclusions of this work and to provide a bird's eye view over the present state of understanding of their LC self-assembly, though not all details are fully understood yet.

3. 4-Cyanoresorcinols as molecules at the rod-banana cross-over

3.1. Synthesis, purification and chemical stability

Though the synthesis of the 4-cyanoresorcinol based BCLCs is straightforward, starting from commercially available 2,4-dihydroxybenzaldehyde and using well established procedures (Scheme 3), it requires some experience to obtain sufficiently pure and long-time stable products. Especially, it must be considered that the CN group



Scheme 3. Synthesis of the 4-cyanoresorcinol derived bent-core mesogens. *Reagents and conditions:* *i:* (1) H₂NOH, (2) Ac₂O; *ii:* NaOH/H₂O; *iii:* (1) **1/n** or **1/m**, SOCl₂, 80°C, 2 hrs, (2) removal of excess SOCl₂, (3) **2/n** or **3** (0.5 equ), DCM, pyridine, 50°C, 2 hrs.; *iv:* H₂/Pd/C; for the structure and abbreviations of the target compounds (see Scheme 2).

increases the reactivity of the adjacent COO groups (especially in position 3) against nucleophilic attack. Such 'active esters' are prone to acyl group transfer, scrambling the COO groups (transesterification) in the molecules not only during synthesis, but also during purification (chromatography and recrystallization), storage and investigation in the temperature ranges of the LC phases. Therefore, the use of common acylation methods with dicyclohexylcarbodiimide (DCC) as a condensation reagent and related reactions, especially those requiring 4-dimethylaminopyridine (DMAP) as acylation catalyst [54], cannot be recommended. Tiny traces of these reagents catalyze the acyl group transfer reactions. This problem is especially serious for molecules involving more than only one type of COO linkage (non-symmetric molecules and multiple COO groups, as compounds **AA**, **AB** and **BB**, see Scheme 2) and involving electron deficit benzoic acids (terephthalates), which additionally enhances the reactivity. Much better is the classical acylation by first activation of the benzoic acids with SOCl_2 or oxalyl chloride to give the benzoyl chloride, careful removal of the excess reagents, followed by reaction with the appropriate phenols with pyridine as base in a second step, which usually leads to pure products being long term stable. Symmetric compounds were simply obtained by acylation of 4-cyanoresorcinol (**3**), whereas non-symmetric compounds require the use of (benzyl)protected 4-cyanoresorcinol (**Bn3**) and a second acylation step of $2/n$ after deprotection (Scheme 3). Table 1 shows typical LC phase sequences observed for the selected representative examples from each series with $Z = \text{H}$ and $m = n = 12$.

3.2. Cybotaxis and local biaxiality in the nematic phases

3.2.1. Cybotaxis

The nematic phases of BCLCs arose significant interest, especially with respect to their potential biaxiality and polar order [53,55–58]. A typical feature of these N phases is cybotaxis (local smectic cluster formation), which was for a long time assumed to represent exclusively a pre-transitional phenomenon [59], but work on bent-core mesogens, especially the 4-cyanoresorcinols [49], 4-halogenated resorcinols [60,61] and oxadiazoles [62–64], has shown that for the nematic phases of these molecules, cybotaxis represents a general feature. The correlation length of these cybotactic clusters increases with growing chain length and decreasing temperature, as confirmed by XRD and dielectric spectroscopy (see Figure 3) [49,65,66]. The usually observed phase type is the skewed cybotactic nematic phase composed of small SmC_s clusters (N_{CybC}), which is characterized by the typical dumbbell shaped diffuse SAXS scattering of magnetically aligned samples [49,62]. The non-tilted SmA type (N_{CybA}) [53,67], showing only one diffuse scattering maximum on the meridian, is only rarely observed. There is still some controversy if the cybotactic clusters represent discrete domains in a continuum of the nematic phase [66], as suggested by cryo-transmission electron microscopy (cryo-TEM) imaging [68,69], or uniform and completely dynamic fluctuating structures with smectic clusters popping in and out of existence, thus combining local smectic with long-range

Table 1. LC phases and transition temperatures of selected 4-cyanoresorcinol based BCLCs with either two alkyl (n) or alkoxy chains (On).^a

Comp.	X^1	X^2	Phase transitions ($T/^\circ\text{C}$)	Ref.
II/O12	N=CH	N=CH	Cr 65 SmCP_A 122 SmC 141 SmA 188 Iso	[121]
BB/12	COO	OOC	Cr 93 (SmC_sP_A 70) CybC 103 N_{CybC} 111 Iso	[49]
TT/12	OOC	COO	Cr 114 SmC_aP_A 101 $\text{Sm}(\text{CP})^{\text{hel}}$ 112 SmC_aP_A 113 SmAP_R/SmA 167 Iso	[92]
BT/12	COO	COO	Cr 89 ($\text{Sm}(\text{CP})^{\text{hel}}$ 89) SmAP_R/SmA 142 Iso	[103]
BT/O12	COO	COO	Cr 119 SmAP_R/SmA 162 Iso	[103]
TB/12	OOC	OOC	Cr 87 (SmC_sP_A ($\text{Sm}(\text{CP})^{\text{hel}}$)) 90 $\text{SmC}_s\text{P}_{AR}$ 98 $\text{SmC}_s\text{P}_R^{[\text{sk}]}$ 130 SmA 134 Iso	[103]
TB/O12	OOC	OOC	Cr 114 (SmC_sP_A 106 $\text{SmC}_s\text{P}_{AR}$) 116 $\text{SmC}_s\text{P}_R^{[\text{sk}]}$ 148 Iso	[103]
AA/O12	N=N	N=N	Cr 71 (SmC_sP_A 70) M_1 75 $\text{SmC}_s\text{P}_{AR}$ 83 $\text{SmC}_s\text{P}_R^{[\text{sk}]}$ 96 SmC_s 127 N_{CybC} 137 Iso	[98]
AT/O12-O14	N=N	COO	Cr 82 (SmC_sP_A 82) SmC_sP_A 111 $\text{SmC}_s\text{P}_{AR}$ 115 $\text{SmC}_s^{[\text{sk}]}$ 145 SmA 164 Iso	[103]
AB/O12-O14	N=N	OOC	Cr 126 (SmC_sP_A 67 SmC_sP_A 77 $\text{SmC}_s\text{P}_{AR}$ 82 SmC_s 89 N_{CybC} 117) Iso	[103]

^a Z^1 and $Z^2 = \text{H}$. Phase abbreviations follow the general recommendations for LC phases, less common abbreviations: CybC = intermediate mesophase with SmC_s -domain structure, which cannot unambiguously be assigned to either SmC_s or N_{CybC} and SmC_sP_A is a polar smectic phase with residual polar domain structure; $\text{Sm}(\text{CP})^{\text{hel}}$ = short pitch heliconical polar SmC phase (previously also abbreviated as SmCP_a , $\text{Sm}(\text{CP})_a$ and $\text{SmC}_s\text{P}_F^{\text{hel}}$), if given in () it is a metastable (monotropic) phase, if shown between {and} it is a long time persistent phase being induced by a pulsed E-field; $\text{SmAP}_R/\text{SmC}_s\text{P}_R$ = polarization randomized (paraelectric) ranges of the SmA/SmC_s phases; $[\text{sk}]$ indicates the formation of a conglomerate of chiral domains in the LC phase, observed in thin films between glass substrates; $\text{SmC}_s\text{P}_{AR}$ indicates a synclinal tilted (super)paraelectric phase showing double peak switching in ITO cells and ferroelectric switching in freely suspended films; M_1 and SmC_sP_A are polarization modulated phases with unknown or modulated SmC structure, respectively. The SmA phases are all de Vries type.

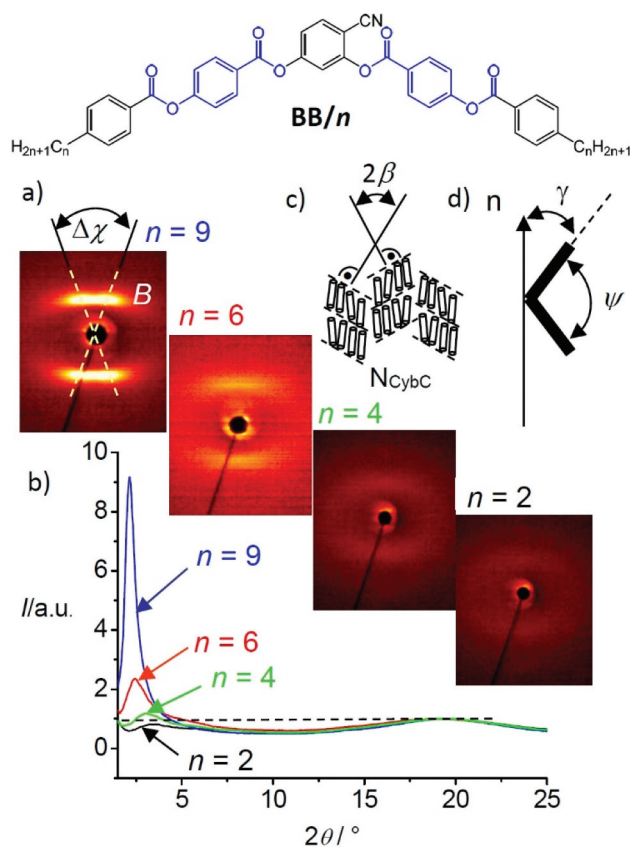


Figure 3. (a) 2D SAXS patterns of magnetically aligned samples in the N_{Cybc} phases of compounds **BB/n** depending on chain length and on temperature, (b) their SAXS plots with (c) model of the molecular organization in the N_{Cybc} phases and (d) explanation of the alignment of the molecules under the applied magnetic field. Reprinted from ref. [49], copyright 2010, RSC.

nematic order. We prefer the second view and assume that only after cryo-treatment, discrete clusters become fixed and then can be observed on a mesoscopic level.

These dynamic clusters give rise to a change of macroscopic properties, such as an increased viscosity of these nematic phases [70] and special elastic and flexoelectric properties [71,72]. For example, for **BB/O12**, the bend elastic constant k_{33} was found to be much smaller than the splay elastic constant k_{11} in the whole temperature range [73] due to the twisted and bend molecular shape [74]. This allows the preparation of mixtures with typical N_{TB} forming materials such as **NCnCN** (Scheme 1) retaining the N_{TB} phase in these mixtures up to relatively high concentrations of the 4-cyanoresorcinol based compound [75]. Under an applied electric field the formation of striped electro-convection patterns [55,76,77] is a common feature of the bent-core nematic phases. Sometimes, the distance between the convection roles becomes so small that it is in the range of visible wave length, and then, the texture

appears like a fan-texture of a planar aligned smectic phase [55]. In some cases, an inversion of the dielectric anisotropy ($\Delta\epsilon$) depending on chain length and temperature is observed [65,70,78]. For example, for the compounds **BB/n** (Figure 3), $\Delta\epsilon$ is positive at high T and negative at low T for the short chain compounds **BB/4 – BB/9** and always negative for **BB/10** with long chains. The negative $\Delta\epsilon$ is due to the hindrance of the rotation of the individual molecules around their long axes emerging from the local packing in the cybotactic clusters and is observed after exceeding a certain cluster size. This hindered rotation can also support the development of a local polarization within the clusters [55,66] as well as the partial synchronization of molecular conformers [79–81], as will be discussed in Section 4. However, on a macroscopic scale, these effects are canceled out due to the randomization of the domain orientation, leaving only the nematic long-range order [82].

It is noted that the main reason for cybotaxis is not the bend molecular shape, but the relatively large size of the rigid molecular fragments used as building blocks of BCLCs (usually ≥ 5 benzene rings), thus providing a significant source of nano-scale segregation from the flexible alkyl end-chains (rigid-flexible and chemical incompatibilities), which increases with growing chain length [83]. Therefore, it is not surprising that the cybotaxis in nematic phases is a quite general phenomenon which can be observed for any mesogen involving either an extended aromatic core or having any other kind of amphiphilicity, combined with a competing frustration force inhibiting the formation of infinite layers, as for example caused by lateral substituents [84]. In the case of BCLCs, the layer distorting effect is mainly due to the molecular bend and twist, as well as by the developing local polar order which tends to be canceled out by emerging twist, splay or any other kind of layer modulation.

3.2.2. Phase biaxiality

There was a long-lasting debate concerning the potential biaxiality of the nematic phases of BCLCs (Figure 4), and it is now common sense that phase biaxiality is unlikely to arise directly from the bent molecular shape of the individual molecules. Instead, it might be a result of the local SmC_s (or SmC_sP_F) cluster structure of the cybotactic nematic phases, providing an increase of the rotational barrier around the long axis. However, this biaxiality develops only within the clusters which are still randomized on a larger scale [49,85,86]. As the cluster size increases with lowering temperature and growing alkyl chain length, there could, in principle, be a critical cluster size above which their coupling leads to macroscopic phase biaxiality, even before the transition to the smectic phase takes place.

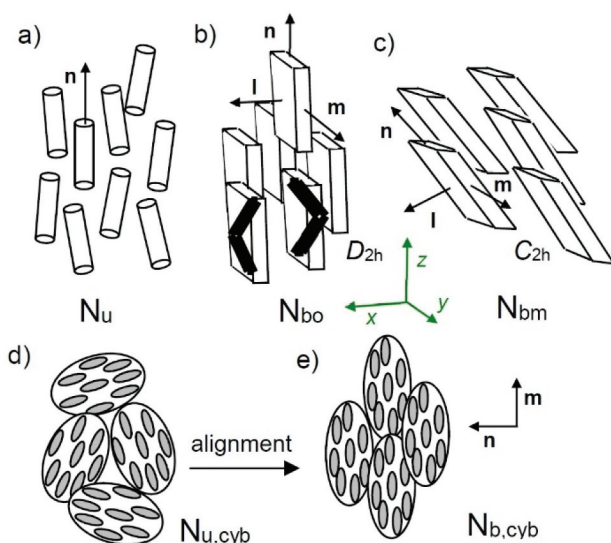


Figure 4. Nematic phases of bent-core molecules: (a) uniaxial nematic phase of molecules rotationally disordered around their long axis (N_u), (b) restricted rotation around \mathbf{n} , but without polar order, leads to the orthorhombic D_{2h} symmetry (N_{bo} phase), (c) biaxial nematic phase with monoclinic C_{2h} symmetry (N_{bm} phase), and (d,e) clusters where the view is along direction z of the reference system; (d) rotationally disordered biaxial clusters, leading to uniaxiality; (e) phase biaxiality due to alignment of the biaxial clusters. Reprinted from ref. [53], copyright 2010, RSC.

However, it is difficult to distinguish a spontaneous phase biaxiality from an induced biaxial state due to the influence of surface interactions, electric [87] or magnetic fields, or any other external stimuli occurring under the measurement conditions. An example of biaxiality in the nematic range was observed by optical investigations of compound **BB/6-12** (see Fig. S1) with two differently long alkyl end-chains, just before the transition to the SmC_s phase in a small temperature range of the N_{CybC} phase [88]. It is noted that this is obviously not due to a transition to a smectic phase as no DSC peak is associated with the onset of biaxiality and that XRD studies confirm the absence of a layer scattering. The SAXS is still diffuse with a continuously growing correlation length across this temperature range. Because these data were not included in the original paper, they were added to the supporting information of this article as Fig. S1. It is proposed that in this case the surface aligns the minor (secondary) director \mathbf{m} along the rubbing direction and by applying an in-plane field the director \mathbf{m} follows the direction of the applied electric field [88]. Thus, under these conditions, this cybotactic nematic phase range with relatively large SmC_s clusters assumes a monoclinic biaxial nematic state (N_{bm} , Figure 4(c)). The reason for this observation might be associated with the large cluster size and the suppression of the transition to a long-range smectic phase by the very different chain

length at both ends [89]. It is likely that in mixtures the temperature range of the biaxial nematic state can be further expanded.

Though it was tried hard, there is presently no indication of the orthorhombic type of biaxial nematic phase or state (N_{bo}) derived from the N_{CybA} phase (Figure 4(b)) [53]. One reason is that non-tilted LC phases are rare for bent molecules [53,67]. Moreover, the SmA phases of bent-core mesogens can be considered as de Vries-like SmA phases formed by SmC_s clusters being too small to assume a long-range uniform alignment of the tilt direction [47,90–92]. In line with the de Vries character, a typical feature of these SmA phases of bent-core molecules (which in fact represent SmC_s phases with short range tilt correlation) is the absence of a change of the d -spacing at the SmA - SmC_s transitions. Due to the smaller tilt and cluster size, the randomization of the secondary director is much easier than in the N_{CybC} phase.

3. 3. Nematic to smectic transitions

The N_{CybA} - SmA and N_{CybC} - SmC_s transitions on cooling are more complicated than the N - Sm transition known for classical rod-like mesogens as the clusters are so dominant and continuously or stepwise grow on cooling. Moreover, the clusters can assume different shapes (oblate, prolate and ribbon-like) and develop local polar order [49]. Therefore, often additional intermediate phases emerge via continuous phase transitions or transitions with very small enthalpies. Among them, cluster phases that were tentatively designated as $CybC$ / $CybA$ and cannot be unambiguously assigned to either nematic or smectic phases (e.g. by the SAXS line width) are considered to be composed of giant clusters [49,93]. Sometimes the low temperature ranges of the N_{CybC} phases mimic textures of biaxial nematic phases [94] and N_{TB} phases [32,95]. However, in order to identify any N_{TB} -like twisted intermediate phases, confirmation of the helical structure by at least one appropriate method (TEM [69] or resonant soft X-ray scattering, RSoXS [96,97]) would be required.

3. 4. Development of tilt and polar order in the smectic phases of azobenzenes AA/On and AAF/On

Figure 5 shows the typical chain length and temperature dependence of the phase transitions of 4-cyanoresorcinol based BCLCs for two series of compounds containing two azobenzene wings as examples. Compounds **AA/On** have relatively electron rich wing groups with a strong driving force for uniform tilt ($\sim 30^\circ$) and forming exclusively

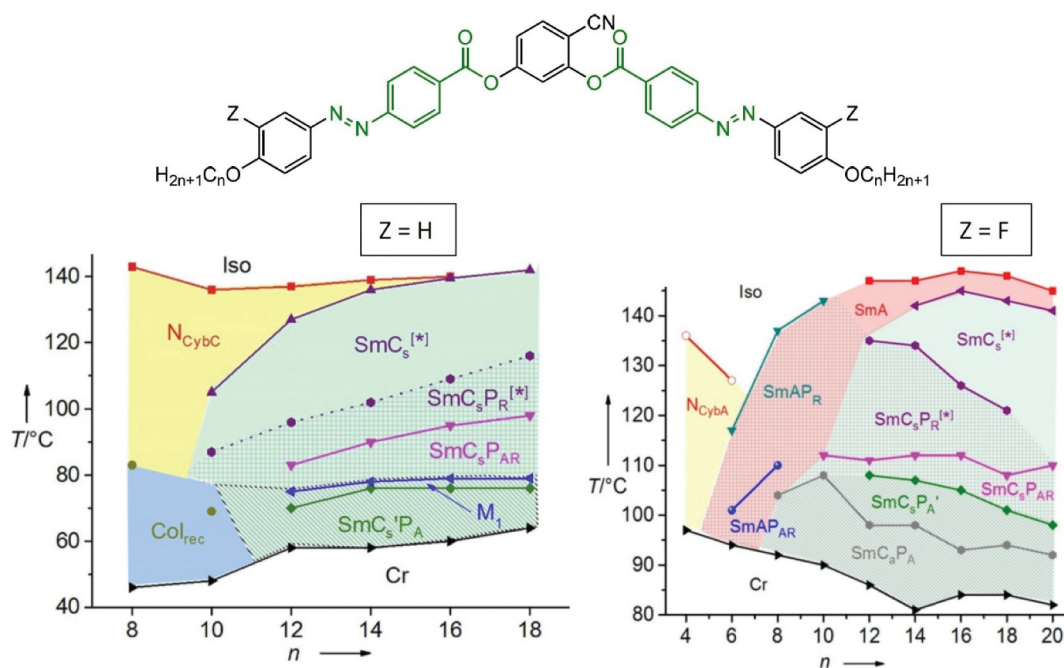


Figure 5. Effect of chain length and temperature on the phase types and phase sequences of (a) compounds **AA/On** with two identical azobenzene wings and (b) the related peripheral wing-fluorinated compounds **AAF/On** [98,100]. Reprinted from ref. [100], copyright 2016, Wiley-VCH.

synclinal tilted N_{Cybc} and SmC_s phases (besides Col_{rec} , Figure 5(a)) [98,99]. The series of fluorinated compounds **AAF/On**, (Figure 5(b)) having reduced electron density in the wings due to the electron withdrawing F atoms at the periphery, shows a reduced tilt ($\sim 15\text{--}20^\circ$) [100,101]. This enables the formation of N_{CybA} and SmA phases for the short chain compounds; the SmA phase even persists for long alkyl chains in certain T -ranges, and there is an additional transition from synclinal to anticlinal tilt in the polar antiferroelectric $SmCP_A$ phases at lowest temperature. In both homologous series, the synclinal tilt becomes more dominating with growing chain length, though the tilt angle itself does not change significantly. For the effects of other fluorination patterns, see ref. [100].

Similar phase sequences were found for the series **AB**, **BB**, **AT**, **BT**, **TB** and **TT** involving only one azo group or exclusively COO linking units (Table 1). The compounds having one or both azobenzenes of compounds **AA** replaced by the electron rich phenyl benzoate wing (**AB**, **BB**) show even lower phase stability and exclusively strongly tilted phases [49,102], whereas those involving at least one electron deficit phenyl terephthalate unit (**TT**, **AT**, **BT**, **TB**) show much higher isotropization temperatures, a smaller tilt and have a SmA high temperature phase [92,102,103]. Details of these series are described in the references given in Table 1; the terephthalates **TT** will be discussed in the following sections in more detail.

3. 5. Development of polar order in the smectic phases of terephthalates **TT/n** and **TT/On**

The development of polar order was in detail studied for compound **TT/O6**, having two electron deficit terephthalate based wings (Figure 6(a–c) [108] which strengthen the attractive core-core interactions and lead to smaller tilt angles and much higher $LC \rightarrow Iso$ transition temperatures compared to the related benzoates **BB/On** and **BB/n**, forming predominately synclinal tilted N_{Cybc} and SmC phases (compare **BB/12** and **TT/12** in Table 1, $\Delta T \sim 56^\circ C$). For the short chain compounds of this series local polarization develops already in the SmA phases as indicated by the emergence of a small and relatively broad single polarization current peak ($SmAP_R$, Figure 6(d)) [10,104–106]. Upon further cooling, this single peak is replaced by two broad and widely separated polarization current peaks ($SmAP_{AR}$, Figure 6(e)) [107], which become sharp while approaching to each other on further cooling at the transition to the polar smectic phase which assumes an anticlinal tilt (SmC_aP_A , Figure 6(f)). Increasing dielectric permittivity and second harmonic generation (SHG) intensity under an applied E-field confirm the growth of polar domains, increasing in coherence length with lowering temperature while simultaneously the polarization in the domains grows [108]. For small grains polarization works against thermal agitation, giving rise to an overall

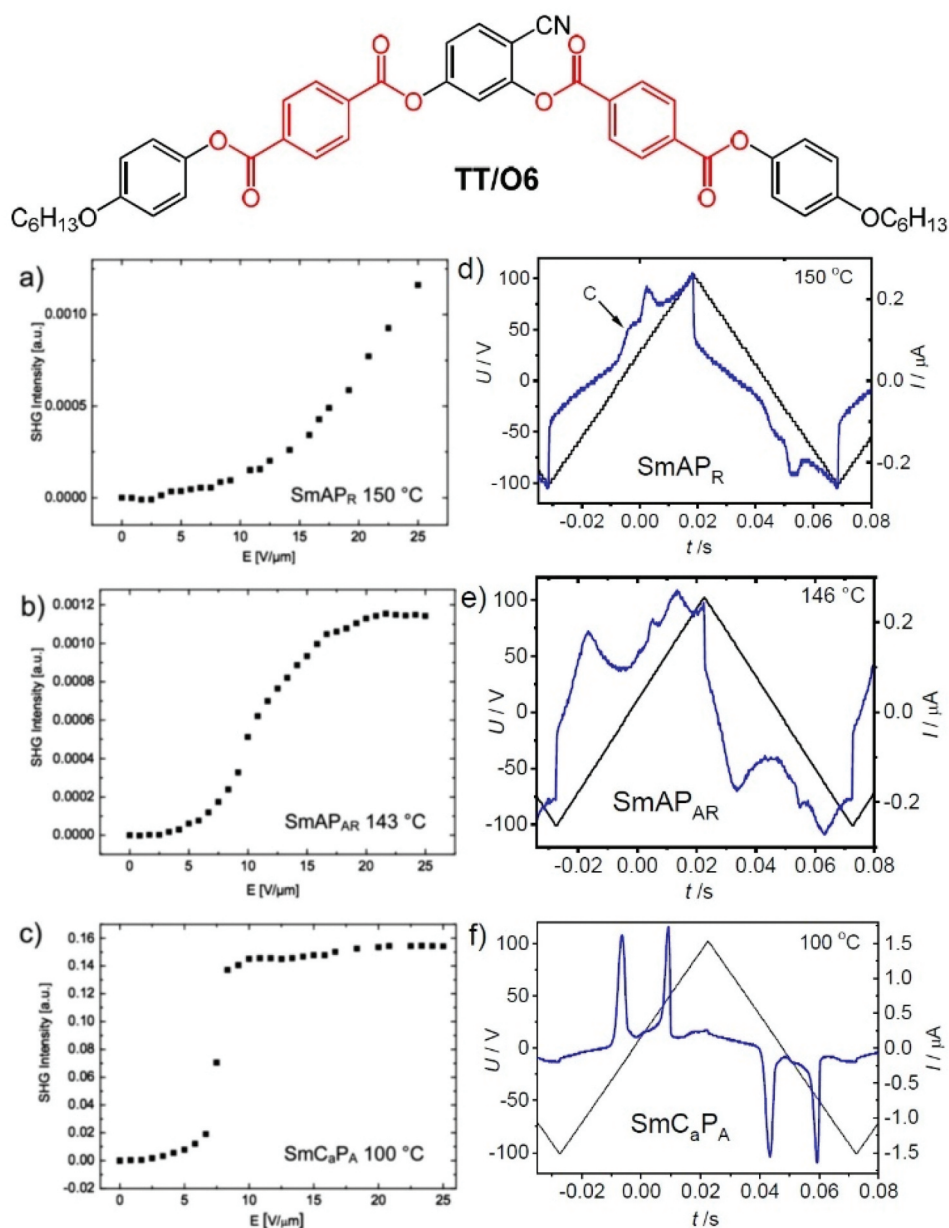


Figure 6. Field-dependence of the SHG signal (left) and polarization current curves under a triangular wave voltage (200 Vpp, 10 Hz, 6 μm ITO cell, right) of compound **TT/O6** depending on temperature (a,d) SmAP_R range (c is most likely a conductivity peak); (b,e) SmAP_{AR} range of the SmA phase (in (e) there is still a small residual peak from SmAP_R) and (c,f) SmC_aP_A phase, the sharp double peaks in (f) and the discontinuous field-dependence in (c) demonstrate the AF character of the switching. Reprinted from ref. [108], copyright 2017, Wiley-VCH.

apolar phase with paraelectric behavior (SmAP_R). In an electric field the antipolar order is easily distorted leading to a strong electric polarizability. The relatively broad size distribution of the small domains gives rise to a broad distribution of the switching energy and to wide current response peaks (Figure 6(d,e)). Emerging polar order is also manifested in the strong increase of the SHG signal in response to an external electric field

(Figure 6(a-c)). With growing domain size the antipolar correlation is strengthened and a transition from a single polarization peak in the SmAP_R range to two broad peaks in the SmAP_{AR} range of the paraelectric phase is observed (Figure 6(b,e)). Nucleation of the AF phase at a critical size of the polar domains is indicated by the transition to two sharp peaks (Figure 6(c,f)) at the transition from a continuous Langevin-type

polarization process to the antiferroelectric switching. Overall, the development of polar order in the SmA phase is a continuous process, so that no visible enthalpy is associated with it (erroneously an enthalpy was reported for the continuous SmA-SmAP_R transition of **TT/12** [113]; this was correct in ref. [92], showing the correct DSC traces). Therefore, SmAP_R and SmAP_{AR} are considered as distinct ranges of the same SmA phase; only the transition to the polar and tilted SmC_aP_A phase is in all cases associated with a small transition enthalpy of around 0.5 kJ mol⁻¹ [92].

3.6. The general phase sequence and intermediate phases

The sequence SmAP_R-SmAP_{AR}-SmC_aP_A is observed for all other 4-cyanoresorcinol based BCLCs with at least one electron deficit wing (**TT/n**, **BT/n** and **AAF/On**) and relatively short alkyl chains. For homologues with longer chains, biaxiality develops first and the transition from apolar via paraelectric to polar smectic phases takes place within the synclinc SmC_s range (see Figure 5(b)). This leads to SmC_sP_R and SmC_sP_{AR} ranges [98], representing new biaxial analogues of the previously known uniaxial SmAP_R and SmAP_{AR} ranges of the SmA phase [105–107]. In addition, the anticlinic SmC_aP_A phase is fully or partly replaced by the synclinc SmC_sP_A phase.

Considering the de Vries character of the SmA phases of most BCLCs, it is likely that local tilt is already present in the uniaxial paraelectric SmAP_{(A)R} ranges and the domain size exceeds the critical length for long-range tilt correlation in the biaxial SmC_sP_{(A)R} phases. It is noted that the SmC_sP_{AR} range of the paraelectric SmC_s phase was first thought to be a ferroelectric SmC_sP_F phase, because in freely suspended films, the

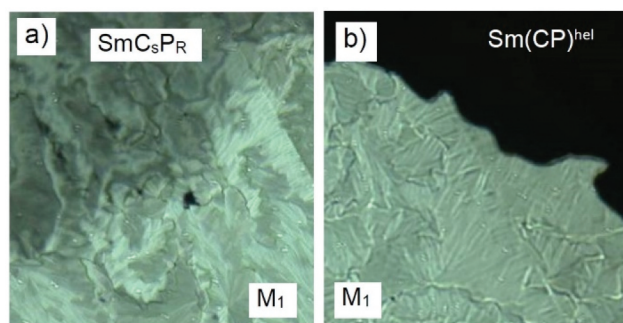


Figure 7. Texture showing the coexistence of the M₁-phase of compound **TT/O14** with (a) the SmC_sP_R phase at $T = 133^\circ\text{C}$ and (b) with the uniaxial heliconical Sm(CP)^{hel} phase at $T = 130.5^\circ\text{C}$ as observed on cooling in a homeotropic 8 μm cell. Reprinted from ref. [110], copyright 2014, RSC.

switching was experimentally found to be bistable (ferroelectric) [98]. However, it appears that the growing polar domains tend to assume an antipolar modulation which is suppressed in the freely suspended films (SmC_sP_F) and supported by the strong surface anchoring on glass substrates (SmC_sP_{AR}). This antipolar modulation can obviously also lead to the emergence of new modulated phases (M₁/SmC_sP_A, Figures 7,8) emerging at the SmC_sP_{AR}→SmC_sP_A transition of compounds with relatively strong tilt. The development of layer modulation can be deduced from a change of the texture from fan-like to mosaic-like, associated with a substantial increase of viscosity (Figure 7). However, it is difficult to detect any additional periodicity by SAXS, even by using a synchrotron source [110]. Therefore, the precise structure of these intermediate phases, tentatively designated as M₁ or SmC_sP_A (which both might be identical or not), is still unclear. Upon further cooling, these phases transform into undistorted smectic phases with flat layers after assuming a strict antipolar order.

The phase sequences observed for most investigated 4-cyanoresorcinol derived BCLCs depending on tilt correlation and temperature are summarized in Figure 8 [98–103,108–111]. It is recognized that the modulated phases occur only for molecules forming strongly tilted SmC_s phases (left hand side of Figure 8), whereas compounds with smaller tilt and involving an SmA phase (blue) at higher temperature and an anticlinic SmC_sP_A phase (green) at low T (right hand side of Figure 8) form heliconical intermediate phases (Sm(CP)^{hel}) instead; this will be discussed in Section 4.1.

3.7. Synclinc vs. anticlinic tilt

In the SmC phases of the weakly bent 4-cyanoresorcinols the electric field induced switching typically takes place by rotation around the long axis (Figure 9(a), left), inverting the layer chirality, but retaining the orientation of the optical axis [112]. The easy rotation of the 4-cyanoresorcinols around their long axes also provides an almost rod-like average shape of the molecules. The fluctuations of these rotational disordered molecules between the layers contributes to a synclinc longitudinal coupling between adjacent layers, whereas within the layers this rotation restricts the coherence length of polarization (Figure 9(b), left). Therefore, paraelectric phases composed of synclinc tilted polar domains (SmC_sP_F) are typically observed. With decreasing temperature and growing molecular bend the energy barrier for the rotation around the molecular long axis is increased, strengthening the polar coupling within the layers and simultaneously reducing the fluctuations

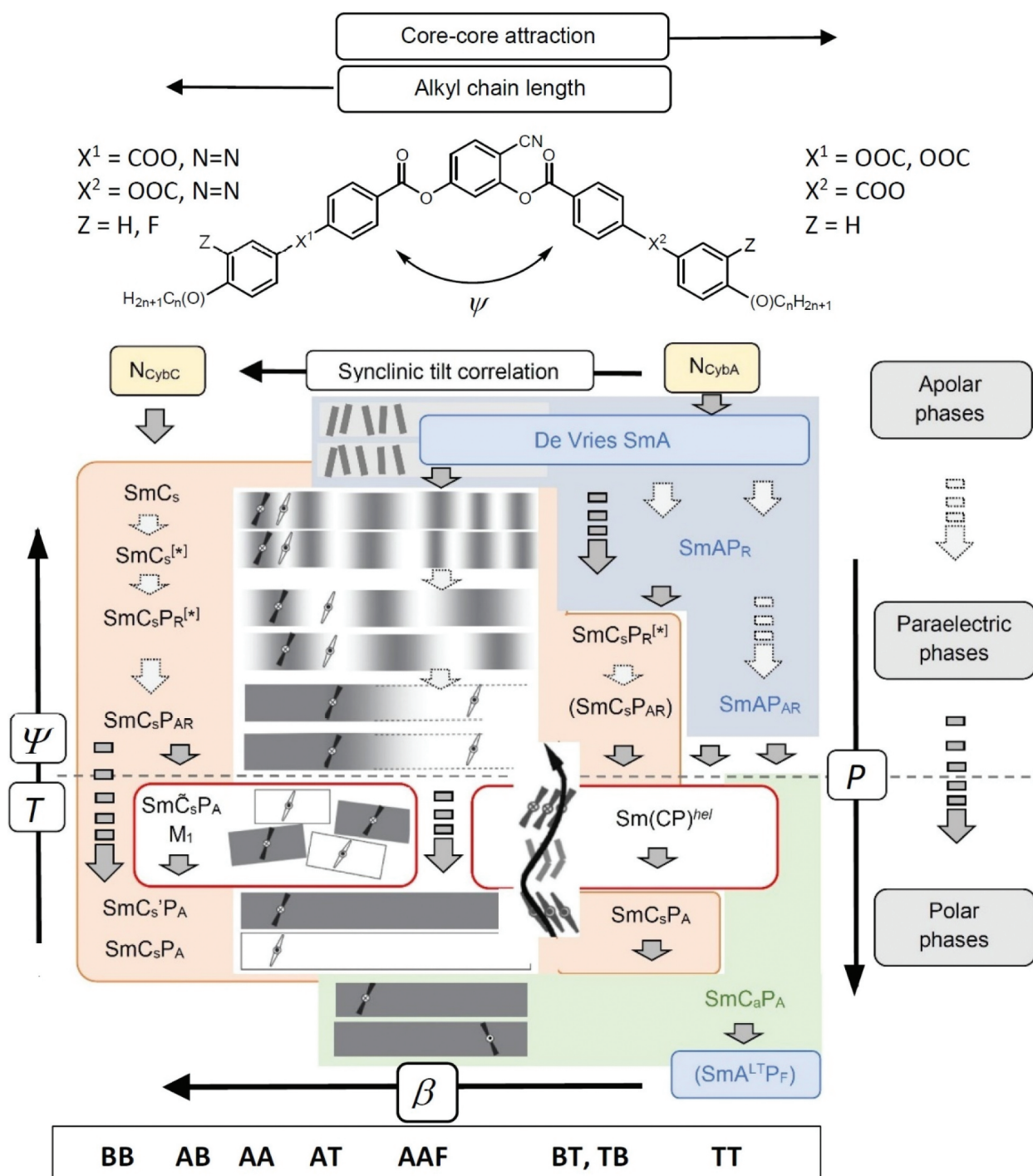


Figure 8. Development of tilt, tilt correlation and polar order (P) in the LC phases of BCLCs at the cross-over between linear and bent molecular shapes, depending on temperature (T), molecular opening angle (ψ) and molecular structure; dark gray arrows indicate phase transition, light gray arrows refer to changing polar order in the same phase; non-tilted phases are indicated in blue, synclinc in red and anticlinic in green. At the bottom, the phase sequences are associated to typical series of 4-cyanoresorcinol based BCLCs (see Scheme 2).

between the layers. Thus, the driving force for synclinc packing is reduced and simultaneously the fluctuations between the rod-like wings of the antipolar packed bent aromatic cores become more dominating (Figure 9(b), right). This supports the development of antipolar

coupling between the layers with further growing polarization of the layers at lower temperature. Though the rotational barrier is increased in the polar phases the switching still takes place by collective rotation around the long axis (as long as there is no helix formation, see

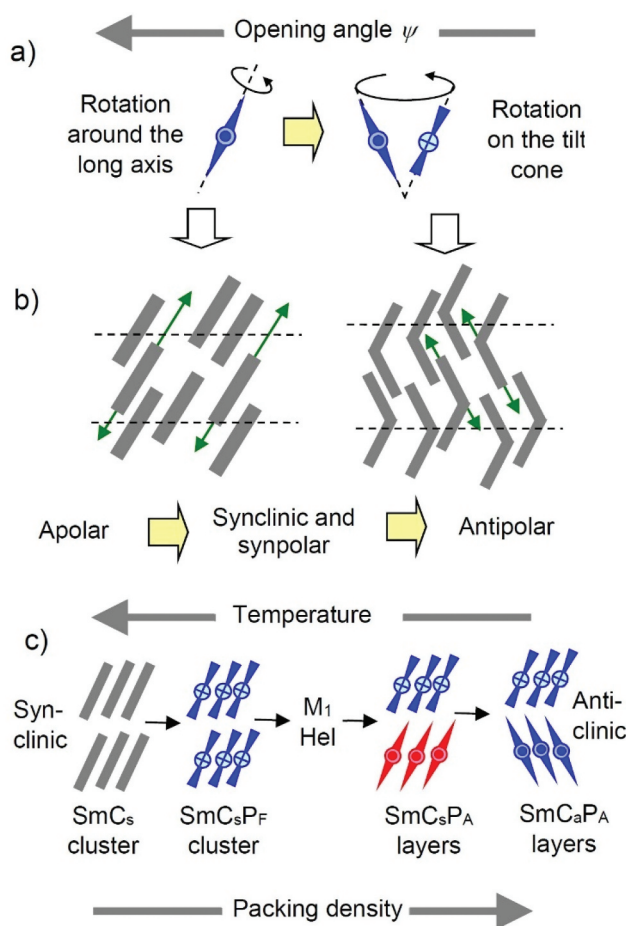


Figure 9. Effects of the opening angle and the molecular rotation on (a) the switching process and (b) the out-of-layer fluctuations (green arrows); (c) the structure of tilted smectic phases formed by molecules with a shape at the transition between linear and bent.

Section 4). As summarized in Figure 8, compounds with strong tilt (**AA/On**, **BB/n**, **BB/On**, Figure 5(a)) [43,49,92] have only synclincic paraelectric and polar smectic phases, compounds with intermediate tilt (**AT/n**, **AAF/On**, Figure 5(b)) show a synclincic to anticlincic transition in the polar smectic range, whereas compounds with even smaller tilt (**TT/n**, with $n < 14$, Figure 10(a)) show the sequence $\text{SmAP}_R \rightarrow \text{SmAP}_{AR} \rightarrow \text{SmC}_a\text{P}_A$ without any synclincic phase (Figure 6). The strength of tilt depends on the molecular structure, where electron deficit cores disfavor the tilt and elongation of the alkyl chain supports the synclincic tilt.

3.8. The SmC_dP_A phase of low tilt compounds

The relations between chain length and LC phase type is shown in Figure 10(a) for the series of compounds **TT/n**. All compounds with $n \geq 6$ have a transition from SmAP_R via SmAP_{AR} to polar smectic phases, being

either anticlincic tilted (SmC_aP_A) for compounds with n up to $n = 16$, or synclincic tilted (SmC_sP_A) for those with longer chains ($n \geq 18$). The emergence of tilt at the $\text{SmAP}_{(A)R} \rightarrow \text{SmC}_a\text{P}_A$ transition is difficult to detect by optical or XRD investigation, because the tilt is relatively small and anticlincic, the switching in planar cells takes place by rotation around the long axis (no tilt or rotation of the extinction crosses is observed) and the layer spacing almost continuously increases on cooling without any discontinuity across the $\text{SmAP}_{(A)R} \rightarrow \text{SmC}_a\text{P}_A$ transition (Figure 11(e)). The growing d -value (despite of the expected decrease!) is at first due to the denser packing which leads to an alkyl chains stretching which more than compensated the layer shrinkage by the emerging tilt. As previously noted, there is already a randomized tilt in the paraelectric SmA phases, actually representing de Vries-like phases, being composed of tilt- and polarization-randomized SmC_sP_F domains. [90,92] These features led in the first instance to an interpretation of these polar smectic phases as non-tilted SmAP_A phases [109,113,114,115–120,122–124]. However, subsequent RSoXS investigations at the ^{13}C -edge indicated the anticlincic tilted character of these biaxial smectic phases (Figure 12(a)) [91] which was rectified in the following up papers [92]. The typical textural feature of these SmC_aP_A phases is a speckled fan texture, which is due to distinct modes of anchoring of the polar direction (bend direction) with respect to the surface (see Figure 11(b) and inset). For compounds with longer chains a synclincic tilt develops before long-range polar order emerges (Figure 10(a)) and the anticlincic SmC_aP_A phase is replaced by the synclincic SmC_sP_A phase for $n > 16$ [92,125]. A reentrance of a non-tilted SmA phase ($\text{SmA}^{\text{LT}}\text{P}_F$) is observed for compounds **TT/16-TT/20** [126], which will be discussed in Section 4.3.

4. Superstructural, supramolecular and transient molecular chirality

4.1. Heliconical smectic phase ($\text{Sm}(\text{CP})^{\text{hel}}$)

The most interesting feature of the series **TT/n** is the formation of a short pitch heliconical smectic phase ($\text{Sm}(\text{CP})^{\text{hel}}$), occurring for compounds with $n > 10$. It is obviously associated with the anticlincic \rightarrow synclincic transition in smectic phases with small tilt and growing synpolar coherence length occurring just as polar order becomes long-range and before it becomes strictly antipolar [92,125,127,128]. The helical pitch P in terms of a number of smectic layers is incommensurate and slightly smaller than 3 times the thickness of a layer, as indicated by the RSoXS experiments (Figure 12(a-c)) [91]. This heliconical smectic phase has first been

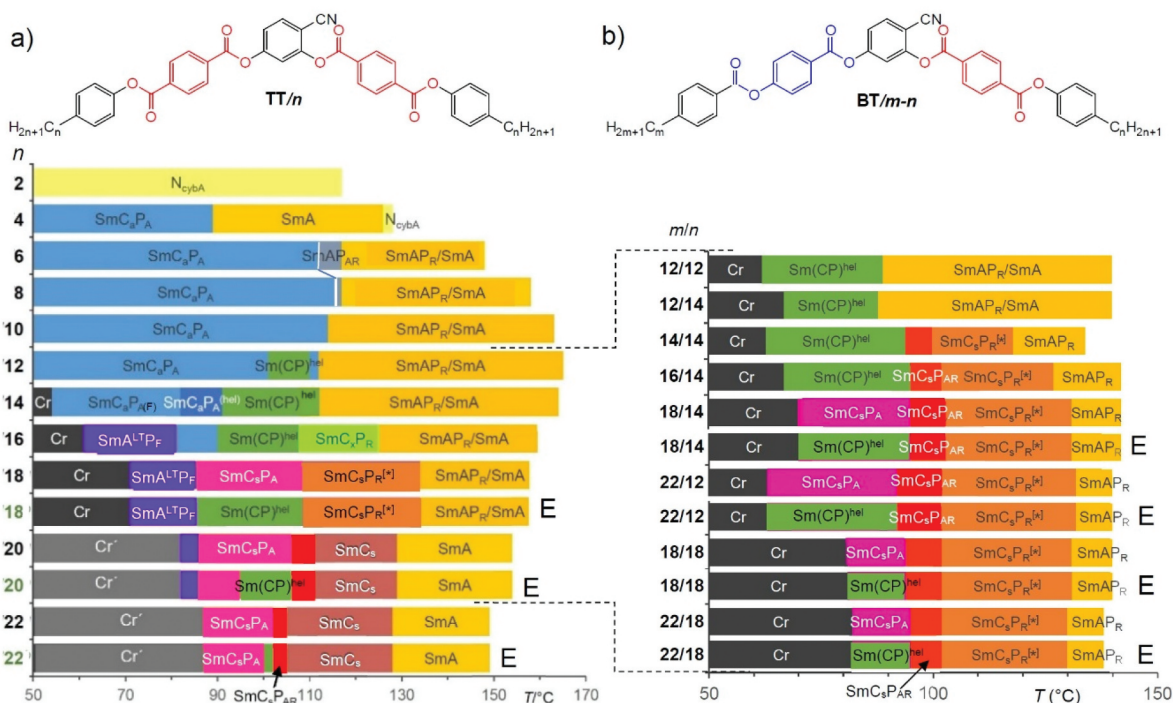


Figure 10. Bar diagrams of compounds (a) **TT/n** and (b) **BT/m-n**, showing the development of the LC phases on cooling and depending on chain length; for the long chain compounds of both series the phase sequence changes after application of a few cycles of an AC field after removing the field; the columns with E show the transitions of these pre-treated samples; abbreviations: $\text{SmC}_s\text{P}_A^{(hel)}$ = SmC_sP_A phase with short-range heliconal structure (though the short range heliconal structure appears to be involved in all SmC_sP_A phases of the series **TT/n**, it is only indicated for **TT/14** where it was proven by RSxS [91]); SmC_sP_R : polarization randomized smectic phase with heliconal structure, $\text{SmA}^{\text{LTP}_F}$ = non-tilted polar low temperature phase; Cr' = crystalline phase with SmA -like texture; for $\text{SmC}_s\text{P}_{A(F)}$ (**TT/14**) AF [92] as well as FE switching [91] was reported, possibly there is a strong dependence on the experimental conditions for this compound at the borderline between AF (SmC_sP_A) and FE ($\text{SmA}^{\text{LTP}_F}$) phases (see Table 1 for other abbreviations) [92,103]. a) is adapted from Ref. [92]; an expanded version is shown in Fig. S4 in the SI.

assumed to be an orthogonal SmAP_α phase where the polar direction changes by a uniform angle unequal to 0° or 180° between the polar layers [129]. Later, it was recognized that there is a small tilt which sets in together with the polar order (SmCP_α) [110]. The present designation is either $\text{SmC}_s\text{P}_F^{hel}$ [127], $\text{Sm}(\text{CP})_\alpha$ [91] or $\text{Sm}(\text{CP})^{hel}$, the latter is use herein [92]. A typical feature associated with the $\text{Sm}(\text{CP})^{hel}$ phase, indicating the tilted organization, is the formation of a field-induced so-called tiger stripe texture (Figure 13(b,e,h)) [91,92] which is attributed to the partial unwinding of the helix under the applied electric field and formation of a striped SmC_sP_F multidomain texture with alternating tilt direction. Further increasing the field strength then leads to larger polar domains in the typical macroscopic tilt domain texture (Figure 13(c,f,i)) after complete removal of the helix. The polarization current curves under a triangular wave field are condition dependent. Often two peaks, the one before 0 V crossing being broader, or three peaks with a pair of close peaks shortly before 0 V crossing and a single peak at higher voltage after 0 V crossing are found (Figure 12(f)). This is

similar to the witching in ferroelectric phases [130,131,132], being in line with the proposed incommensurate triple layer heliconal phase structure.

Without applied field the texture of the $\text{Sm}(\text{CP})^{hel}$ phase appears with the typical features of a SmA phase, indicated by a smooth fan texture and appearing optically isotropic under homeotropic alignment due to the presence of the tight helix parallel to the layer normal (Figure 12(d)). The transition from a speckled to a plain fan texture is a good optical indication of the SmC_sP_A - $\text{Sm}(\text{CP})^{hel}$ transition (Figure 12(d,e)). As shown in Figure 14 typical features of the $\text{Sm}(\text{CP})^{hel}$ phase are high polarization values, a significant dielectric permittivity and field induced SHG activity, in line with a phase formed by large SmC_sP_F domains, being almost completely fused to polar layers. $\Delta\epsilon$ and SHG activity decrease while the polarization further grows after transition to SmC_sP_A when the layer correlation becomes strictly antipolar [92,103].

As shown in Figure 10(a), the $\text{Sm}(\text{CP})^{hel}$ phase appears below a polarization randomized high permittivity SmAP_R , SmAP_{AR} , $\text{SmC}_s\text{P}_{AR}$ or $\text{SmC}_s\text{P}_R^{[*]}$ phase

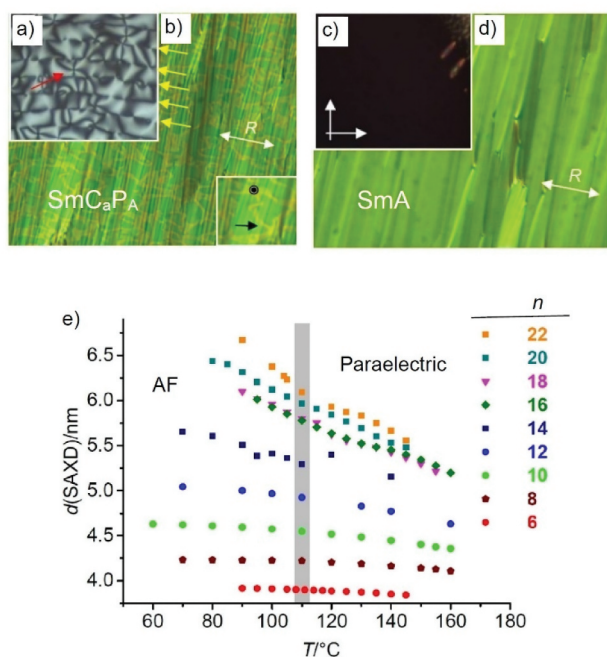


Figure 11. (a-d) Textures of compound **TT/4**, (c, d) in the SmA phase at $T = 118^\circ\text{C}$ and (a, b) in the SmC_aP_A phase at $T = 80^\circ\text{C}$. (a, c) show the homeotropic textures and (b, d) the planar textures; (e) dependence of the layer distance d of compounds **TT/n** on the chain length n and temperature; the grey bar indicates the temperature range of the paraelectric-(anti)ferroelectric transitions. Reprinted from ref. [92], copyright 2020, Wiley-VCH.

and replaces the anticlinic SmC_aP_A phase partly or completely in a certain temperature range slightly below or at the paraelectric-(anti)ferroelectric transition. As the synclinc tilt correlation becomes stronger by chain elongation, the anticlinic SmC_aP_A phase is replaced by the synclinc SmC_sP_A phase for $n = 16, 18$. This phase is achiral and as a result incompatible with helix formation, and as a consequence, the $\text{Sm}(\text{CP})^{\text{hel}}$ phase is removed (see Figure 10(a)). However, the $\text{Sm}(\text{CP})^{\text{hel}}$ phase can still be induced under a pulsed E-field which switches the achiral SmC_sP_A phase to the chiral SmC_sP_F state by rotation around the long axis (Figure 15(e)) [92,103,128]. After switching off the field, the polar layers in the chiral SmC_sP_F state develop a heliconical organization to cancel the polar order. This helix formation is coupled with a (partial) synchronization of helical molecular conformers which in turns leads to a denser overall packing [79]. The helical $\text{Sm}(\text{CP})^{\text{hel}}$ phase once formed cannot relax back to the (racemic) synclinc SmC_sP_A phase due to the diastereomeric coupling between helicity and layer chirality. If the $\text{Sm}(\text{CP})^{\text{hel}}$ phase would relax to the racemic SmC_sP_A phase, for half of the molecules the diastereomeric relations between helix chirality and layer chirality would become unfavourable. This increases the energy barrier

for this transition and therefore, the helix, once formed, is stable after removing the external electric field (Figures 10(a) and 15(e)).

This barrier is smaller for the transition from $\text{Sm}(\text{CP})^{\text{hel}}$ to SmC_aP_A by collective precession on a cone, retaining the layer chirality. Therefore, once the $\text{Sm}(\text{CP})^{\text{hel}}$ phase is formed, the mode of switching changes from the originally preferred chirality inverting rotation around the long axis to a chirality preserving precession on a cone (Figures 9(a) and 15(b-d)) [22,52,133]. The interesting point is, that in this case it is not the degree of molecular bend or a layer modulation which decides about the switching mechanism, but it is the heliconical organization of the molecules, favoring the collective precession on a cone 'kinetically'. Moreover, this process, retaining the layer chirality, retains the lowest energy diastereomeric pair of layer chirality and heliconical twist sense, favoring this process also 'thermodynamically'. The switching process is also voltage dependent and changes to a rotation around the long axis above a threshold voltage required to remove the helix [128]. For intermediate cases more complicated behavior can be found, as for example at the SmC_sP_R - $\text{Sm}(\text{CP})^{\text{hel}}$ transition described in ref. [125].

The $\text{Sm}(\text{CP})^{\text{hel}}$ phase is also observed in the series of compounds **BT/n**, combining an electron deficit terephthalate with an electron rich phenylbenzoate wing [103]. As shown in Figure 10(b), in this series of compounds **BT/m-n**, having different chain length at the ends, the $\text{Sm}(\text{CP})^{\text{hel}}$ phase is stable for the shorter homologues whereas at a certain chain length it is replaced by SmC_sP_A from which the $\text{Sm}(\text{CP})^{\text{hel}}$ phase is obtained as a field-induced phase in the whole SmC_sP_A ranges. It appears that for compounds **BT/m-n** there is a slightly higher tendency to assume a synclinc tilt as indicated by the complete removal of the anticlinic tilted phase in comparison to the same chain length range in the series **TT/n** (see Figure 10, dashed lines). A similar slight shift towards synclinc tilt is also found by replacing one or both alkyl chains by alkoxy chains (**BT/On**) and by flipping the direction of the CN group (**TB/n**, **TB/On** = exchange of the positions of phenyl benzoate and terephthalate wings, see Table 1 for examples and ref. [103] for more details).

The switching of the $\text{Sm}(\text{CP})^{\text{hel}}$ phase is of practical interest for application in electro-optical devices, either using the very fast V-shaped grey scale switching by helix deformation in planar alignment (DHF mode) [123,127,128,134] or the in-plane switching of the secondary optical axis in homeotropic alignment [122,124]. It is remarkable that the switching of the secondary

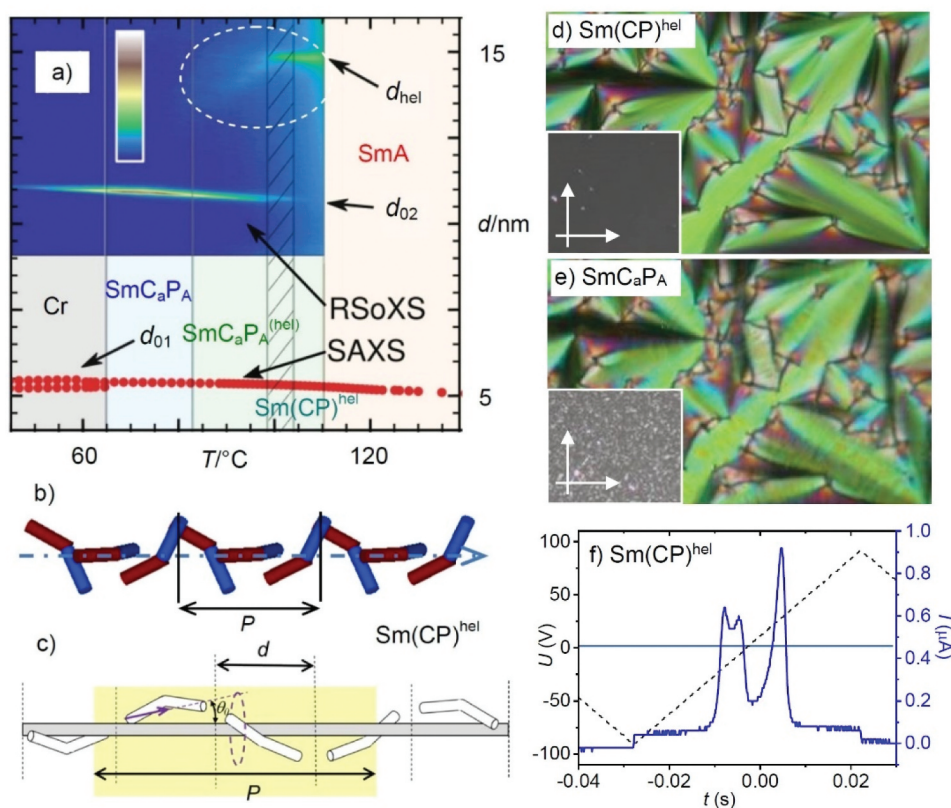


Figure 12. The $\text{Sm}(\text{CP})^{\text{hel}}$ phase. (a) SAXS and RSoXS data in the LC phases of **TT/14** depending on temperature [91]; (b) shows models [128]; (d,e) Textures of compound **BT12/6**; the insets show the corresponding homeotropic textures; (f) polarization current curve of this compound as recorded under a triangular wave voltage at $200 V_{\text{pp}}$, in a $6 \mu\text{m}$ PI-coated ITO cell. (a, b) were reprinted with permission from refs. [91] and [128], respectively, copyright (2019) by the American Physical Society (<https://doi.org/10.1103/PhysRevLett.122.107801>; <https://doi.org/10.1103/PhysRevMaterials.3.045603>).

optical axis in homeotropic samples is not only found in the $\text{Sm}(\text{CP})^{\text{hel}}$ phase itself, but for all compounds **TT/n** in the SmCaP_A ranges [116,118,120]. As shown by RSoXS for **TT/14** [91] (see Figure 12(a)) a residual short-range helix persists even in the SmCaP_A phase ($\text{SmCaP}_A^{\text{(hel)}}$) adjacent to $\text{Sm}(\text{CP})^{\text{hel}}$. This is also responsible for the relatively low birefringence of the homeotropic sample (Figure 16, texture at the left) [92]. As an in-plane electric field with increasing voltage is applied to a homeotropic cell, the birefringence increases first, then it rapidly goes through zero and then rises again (Figure 16). The first increase is attributed to the helix unwinding which leads to a biaxial anticlinic SmCaP_A state and the following changes are in line with an alignment of the secondary director \mathbf{m} while the primary director \mathbf{n} is fixed by the lamellar structure. The intermediate uniaxial state is assumed to result from a 90° twisted tilt correlation between adjacent layers, and this twist angle further decreases until the polar SmC_sP_F state without twist between the layers is reached

[122]. It is noted that the recently reported very similar switching of the secondary director in an anticlinic tilted SmC_a (SmA_b) phase of a bent dimesogen could possibly also be affected by a residual heliconical structure, in this case remaining from the adjacent N_{TB} phase [135].

It is also emphasized that in planar samples, with the field applied between the top and bottom surfaces, the switching in the SmCaP_A range takes place by rotation around the long axis, probably, because the local heliconical twist is suppressed in this alignment [125] (however, in the $\text{Sm}(\text{CP})^{\text{hel}}$ range the heliconical structure is retained in planar alignment, see Figure 13). This observation also suggests that the typical speckled ground state texture of the planar aligned SmCaP_A phase (fan texture) might be interpreted as an indication of a residual driving force for twist between the layers, leading to an alternation of domains with an anchoring of either the polar axis or the bow plane parallel to the surfaces (90° jumps of the alignment of the secondary director in adjacent domains, see inset in Figure 11(b)).

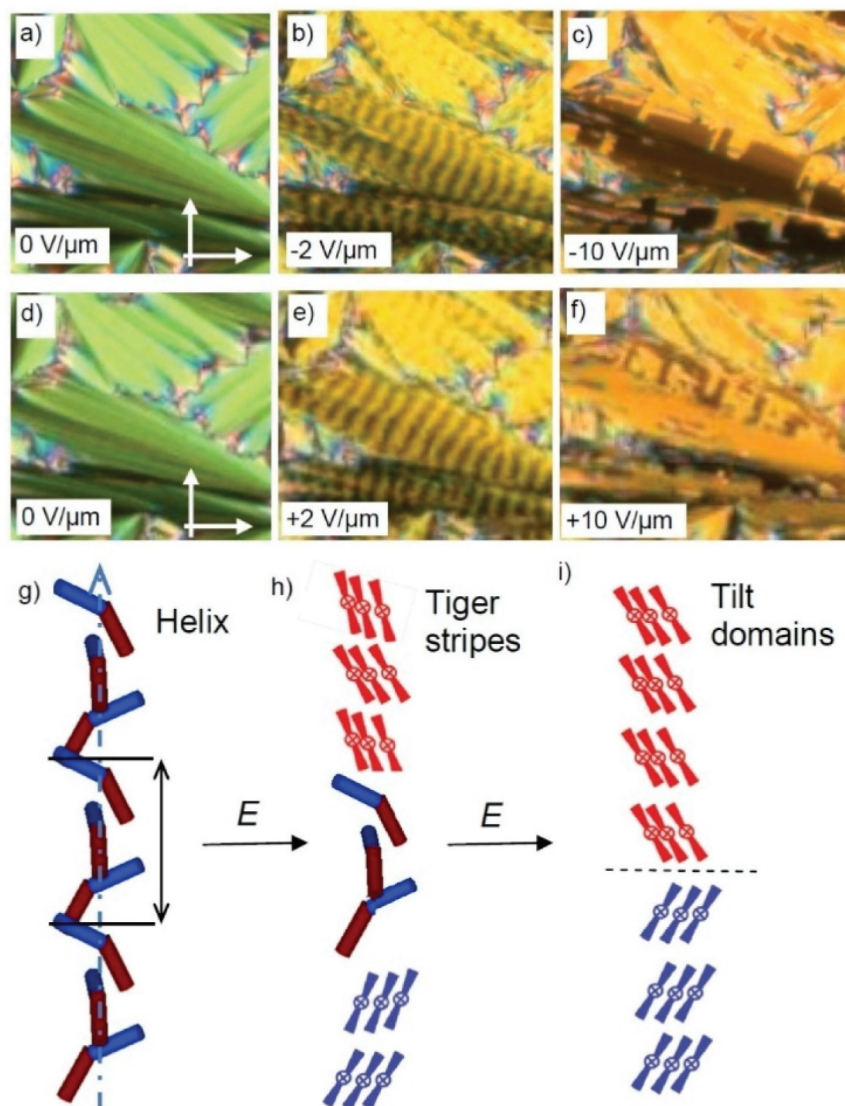


Figure 13. Optical investigation of the switching process of compound **TT/12** in planar alignment (6 μm PI coated ITO cell) under an applied DC field in the $\text{Sm}(\text{CP})^{\text{hel}}$ range at $T = 105^\circ\text{C}$ with models of the distinct field-induced states. Reprinted from ref. [92], copyright 2020, Wiley-VCH.

4.2. Comparison with related heliconical smectic and other mirror symmetry broken smectic and nematic phases

4.2.1. Relations to chiral LC phases of rod-like molecules

Commensurate heliconical phases with 3- or 4-layer pitch were previously known for permanently chiral rod-like molecules in the $\text{SmC}_{\text{FI1}}^*$, $\text{SmC}_{\text{FI2}}^*$ phases, respectively, occurring at the synclinic-anticlinic (= FE-AF = SmC_s^* - SmC_a^*) transition of highly chiral mesogens [131,132]. Likewise, the incommensurate short pitch SmC_α phase was found at the onset of uniform tilt at the SmA^* - SmC^* transition of these

rod-like molecules [136–138]. In this case the permanent molecular chirality, coupling with and biasing the helical molecular conformations is the main driving force of helix formation and the helix sense is fixed by the permanent molecular chirality [139]. For the achiral, but transiently chiral BCLCs very similar heliconical phases appear at the FE-AF transition coinciding with the onset of uniform tilt and the synclinic-anticlinic transition. However, in the $\text{Sm}(\text{CP})^{\text{hel}}$ phase the chirality appears as a broken symmetry, i.e. the developing helix sense is stochastic, assuming either helix sense with the same probability and thus leading to conglomerates (ambidextrous mirror symmetry breaking). Here the

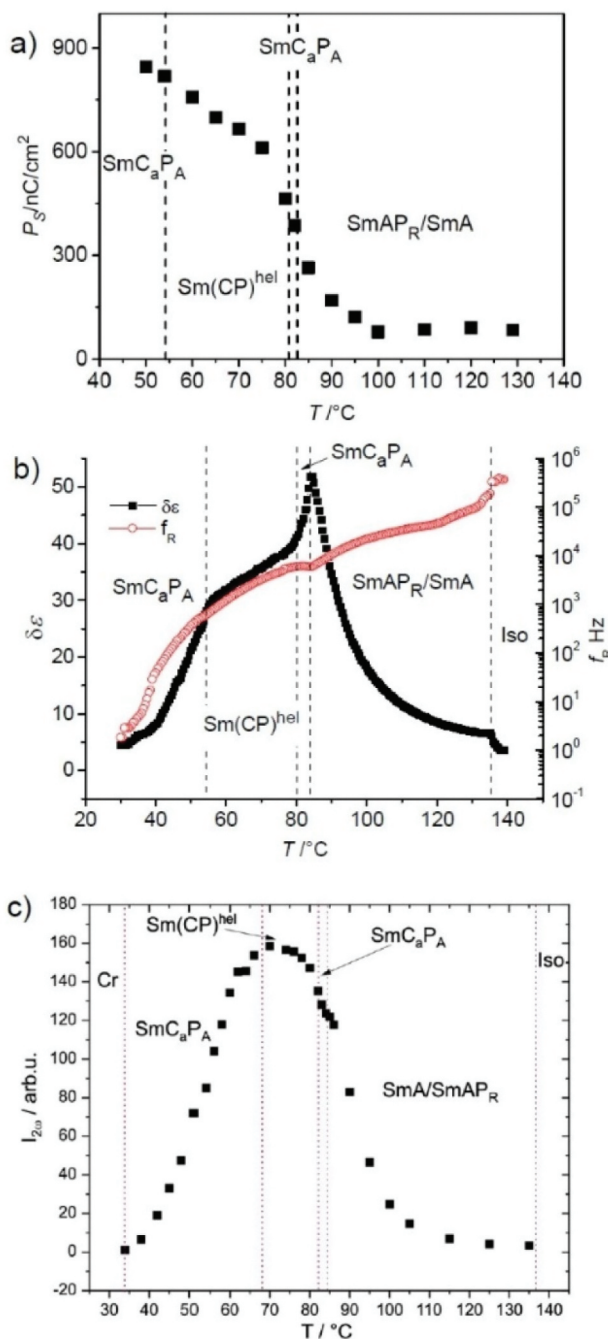


Figure 14. (a) Polarization values (P_s) of **BT/12-6** depending on temperature (Cr 69 $\text{Sm}(\text{CP})^{\text{hel}}$ 81 SmC_aP_A 83 SmAP_R/SmA 131°C Iso) and (b) temperature dependence of the $\delta\epsilon$ and relaxation frequency; (c) shows the temperature dependence of the SHG response $I_{2\omega}$ of compound **BT/18-6** (Cr (SmC_aP_A 69 $\text{Sm}(\text{CP})^{\text{hel}}$ 82 SmC_aP_A 84 SmAP_R/SmA 138°C Iso); the measurements were made on cooling in an AC electric field ($E_{pp} = 25 \text{ V}/\mu\text{m}$) in a $10 \mu\text{m}$ thick IPS cell with ITO electrodes. Reprinted from ref. [103], copyright 2020, RSC.

transient molecular conformational chirality as well as the escape from a developing polar order support the spontaneous helix formation if neither the synclonic nor the anticlinic structure can dominate.

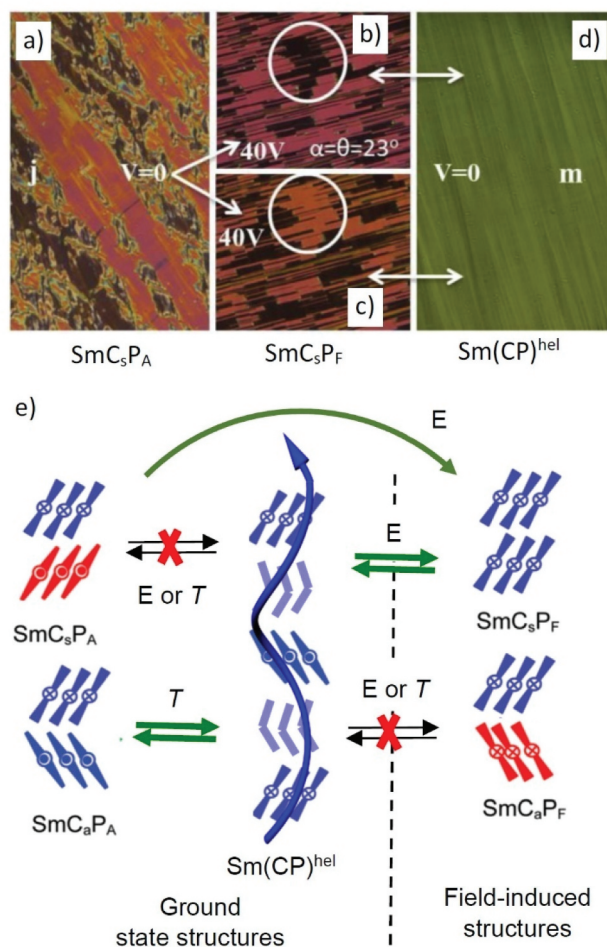


Figure 15. (a-d) Textures of **TT/18** as observed in a planar cell at 100°C , showing the field induced transition of (a) SmC_sP_A to (b,c) SmC_sP_F , followed by relaxation to (d) $\text{Sm}(\text{CP})^{\text{hel}}$ and (b-d) reversible switching between the two SmC_sP_F states and $\text{Sm}(\text{CP})^{\text{hel}}$ at 0 V; (a-d) were used under CC BY 4.0 from ref. [127]. (e) Summary of the field-induced transformations in the polar smectic phases of compounds **TT/n** and **BT/m-n**.

4.2.2. Relations to the SmC_{TB} and N_{TB} phases of bent dimesogens

A non-polar analog of the heliconical $\text{Sm}(\text{CP})^{\text{hel}}$ phase has been theoretically predicted [140,141] and recently found for bent mesogenic dimers below the N_{TB} phase [142]. This SmC_{TB} phase represents a commensurate heliconical phase with 4-layer ($\text{SmC}_{\text{FI2}^*}$ -like) structure with an overlaid larger twist [143]. In other bent dimesogens a biaxial smectic phase is observed below the N_{TB} phase, in which the individual mesogenic cores of the bent dimers are anticlinic tilted [135,143–145]. This phase is related to the SmC_aP_A phase occurring besides the $\text{Sm}(\text{CP})^{\text{hel}}$ phase of the 4-cyanoresorcinol based BCLCs (see Fig. S2). The main difference is the polar order in SmC_aP_A , whereas there is obviously no polar order for the anticlinic smectic phases of the dimesogens.

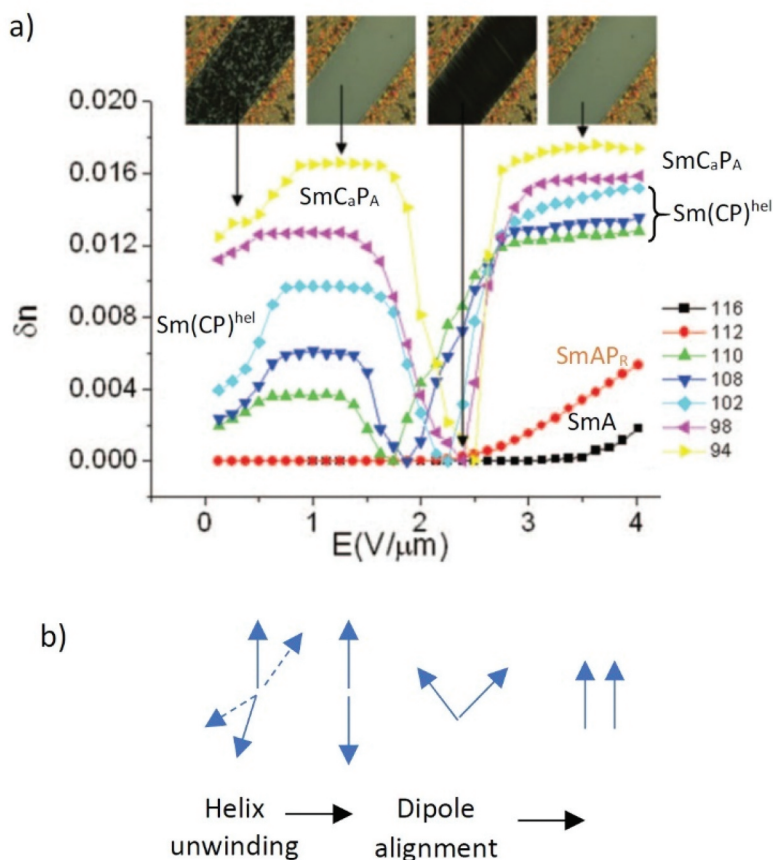


Figure 16. Switching of the secondary director in the SmC_aP_A phases of compounds TT/n . (a) Electric-field dependence of the birefringence δn of $\text{TT}/12$ in a homeotropic cell under an applied in-plane electric field at different temperatures; reproduced with permission from ref. [118], copyright 2012, Taylor & Francis (www.tandfonline.com). (b) shows models of a proposed molecular reorganization under the applied electric field, where the solid arrows indicate the directions of the secondary director in two adjacent layers (dashed arrows represent the next two layers) in a view parallel to the layer normal.

The N_{TB} phase involves only orientational order and heliconical self-assembly, as indicated by NMR spectroscopy [146,147], circular dichroism (CD) [148] and RSoXS [31,149,150]. There is theoretical work showing that the development of the helical twist is entropy driven and only requires a bent, but not any helical molecular conformation (axial chirality) [140]. In line with this, the enantiomeric excess of the molecular conformations within the chiral domains of the conglomerate appears to be relatively small in the N_{TB} phases [151] (though it can become larger in other spontaneously chiral phases, as for example shown for the B4 phase [152]). Nevertheless, there are diastereomeric relations between the transient conformational molecular and the helix chirality, leading to different energies for the diastereomeric pairs. Even if molecular chirality itself would not be required for emergence of chirality, it is likely to support chirality synchronization and helical self-assembly of the molecules. This is in line with results obtained for heliconical phases by mean field theory [141,153]. Overall, chirality synchronization requires a certain coherence

length of molecular order and intermolecular interactions that the free energy gain can exceed the critical value of $\sim 2kT$, as required for chirality synchronization in the liquid state [79,154,155]. Therefore, in the nematic phase cybotaxis-like aggregation with increasing coherence length at reduced temperature might support chiral segregation by increasing the collective coupling of the individual molecules.

4.2.3. Relations to helical network phases

Helix formation and chirality synchronization were also found in LC network phases, as for example in the optically isotropic bicontinuous cubic ($I23$, previously known as ' $Im3m$ ' [156]) and the birefringent 3D tetragonal (SmQ) LC phases [157,158], and it even leads to the mirror symmetry broken isotropic liquids of polycatenar molecules ($\text{Iso}_1^{[*]}$) [155]. In the liquid conglomerates the branching of helical columns provides a long-range transmission of chirality by retaining short-range positional order in the $\text{Iso}_1^{[*]}$ phase and after emergence of a long-range 3D lattice in the cubic ($\text{Cub}^{[*]}/I23$) and

non-cubic (SmQ) phases with 3D lattice, occurring at lower temperature [79,80,159]. It is noted that already about 50 years ago, Ya. B. Zeldovich proposed the existence of a spontaneously chiral isotropic liquid representing the 'minimal LC' with minimal symmetry breaking (only space inversion) [160,161]. This chiral isotropic liquid phase [79,80] completes the sequence of spontaneously mirror symmetry broken LC phases,

$$\text{Iso}_1^{[*]} - \text{N}_{\text{TB}} - \text{Sm}_{\text{TB}} - \text{Sm}(\text{CP})^{\text{hel}},$$

occurring with decreasing phase symmetry by the stepwise emergence of orientational, translational and polar order. In all helical mesophases there is a preference for the side-by-side packing of the molecular/supramolecular helices with the same handedness. The dominance of this *enantiophobic* mode of chiral self-assembly is required for stochastic mirror symmetry breaking leading to the formation of conglomerates by ambidextrous mirror symmetry breaking [79,80,162].

4.2.4. Enantiophilic vs. enantiophobic self-assembly

Interestingly, in crystalline assemblies the *enantiophilic* self-assembly with favourable interaction between opposite enantiomers and leading to *racemates* represent the dominating mode of self-assembly for mixtures of permanently or transiently chiral molecules, observed for >90 % of the cases. In contrast, the *enantiophobic* self-assembly with favourable interaction between like enantiomers and leading to *conglomerates* is rare [163,164]. Helical morphologies are typical for pure enantiomers and conglomerates, whereas the racemates usually form non-helical, often sheet-like structures in the solid state [165]. In LC systems of transient chiral molecules or helical aggregates only the conglomerates are easily recognized by their chiral domain formation or helix formation and therefore dominate the discussion, whereas racemate formation is usually not recognized and their effect on LC self-assembly is therefore underestimated. An example is found in the bicontinuous cubic phases of polycatenar molecules, where enantiophilic packing of two enantiomorphous chiral gyroid networks leads to the achiral (racemic) double gyroid with *Ia3d* space group, whereas enantiophobic self-assembly gives rise to the uniformly chiral *I23* cubic lattice. The transition between *Ia3d* and *I23* takes place by modification of the alkyl chain length as well as depending on temperature [79,158].

4.3. Ferroelectric re-entrant SmA phase ($\text{SmA}^{\text{LT}}\text{P}_{\text{F}}$)

An interesting feature of the long chain compounds of the series TT/n is that the layer spacing of the polar smectic phases increases on cooling more strongly than for those with shorter chains (Figure 11(e)). This is in

line with the experimentally observed decrease of the tilt angle with lowering temperature in the polar smectic phases of the compounds TT/n with $n = 16-22$ [92]. Even a transition to a non-tilted smectic phase ($\text{SmA}^{\text{LT}}\text{P}_{\text{F}}$) is found for these compounds [126], leading to the unusual $\text{SmA}-\text{SmC}_s-\text{SmA}^{\text{LT}}$ phase sequence with a reentrance of the SmA phase on cooling. Formation of an SmA phase below SmC_s has rarely been observed. The few known cases include permanently chiral rod-like molecules and bent mesogenic dimers [166,167]. For compounds TT/n the re-entrant SmA phase is polar. Because only one polarization current peak is observed under a triangular wave voltage, a uniformly polar nature of this $\text{SmA}^{\text{LT}}\text{P}_{\text{F}}$ phase is suggested ($\text{SmA}^{\text{LT}}\text{P}_{\text{F}}$) [92]. In the series of compounds TT/n formation of $\text{SmA}^{\text{LT}}\text{P}_{\text{F}}$ is associated with the anticlinic-synclinic transition upon growing chain length and the $\text{SmA}^{\text{LT}}\text{P}_{\text{F}}$ phase accompanies the heliconical $\text{Sm}(\text{CP})^{\text{hel}}$ phase as a low temperature phase. There must be a specific reason for the very unusual decrease of the tilt upon chain elongation and lowering temperature. Here, it is postulated that in the $\text{Sm}(\text{CP})^{\text{hel}}$ phase the enantiophobic packing, supporting chiral superstructures and conglomerate formation is favored, whereas in the $\text{SmA}^{\text{LT}}\text{P}_{\text{F}}$ range the enantiophilic packing becomes dominating, disfavouring helical and favouring achiral assemblies. This means that chiral phases, either heliconical smectic phases or tilted polar phases with intrinsic layer chirality become disfavoured. For compounds TT/n it leads to the removal of the tilt and a re-entrance of a SmA phase which is non-tilted and achiral. The transition from the chiral $\text{SmC}_s\text{P}_{\text{F}}$ to an achiral leaning phase, described in Section 4.7, can be explained in a similar way, too. The change from enantiophobic to enantiophilic self-assembly could even play a role in the development of either the chiral twist-bend nematic (N_{TB}) [25,25,30-32] or achiral nematic or smectic phases, as for example the achiral splay (N_{S}) and polar nematic phase (N_{F}) [168,169,170-172].

4.4. Surface supported mirror symmetry breaking by conglomerate formation in nematic phases ($\text{N}^{[*]}$)

Mirror symmetry breaking by conglomerate formation was occasionally observed in the nematic phases of BCLCs ($\text{N}^{[*]}$) [173,174]. This was also found for the N_{Cybc} phases of some 4-cyanoresorcinol based BCLCs [175,176] and shown to be due to twisted states developing between the cell surfaces [64,175]. Though this surface supported mode of mirror symmetry breaking would not require any source of chirality, it is assumed to be supported by the pronounced transient helicity of bent-core molecules.

Therefore, it can develop without application of any helical twist between the surfaces and even after linear shearing. The confinement of the molecules in the cybotactic clusters and the chiral SmC_sP_F structure of these clusters can couple with the transient molecular chirality, thus reinforcing its small effect in a cooperative way. The pronounced helicity of BCLC is also known to lead to an increased twisting power induced by chiral dopants, compared with standard rod-like nematic hosts [162]. It is noted that there are alternative explanations only considering the elastic constants. A small twist elastic constants k_{22} [177] or a small or negative bend elastic constant k_{33} are considered as origin of helix formation [26,30], especially if it takes place under confined conditions. In another model a chiral tetrahedral nematic phase with D_2 symmetry was suggested [178,179] which might play a role for nematic phases of short chain BCLCs with low aggregation number or for clusters formed by pairs of bent mesogens [176].

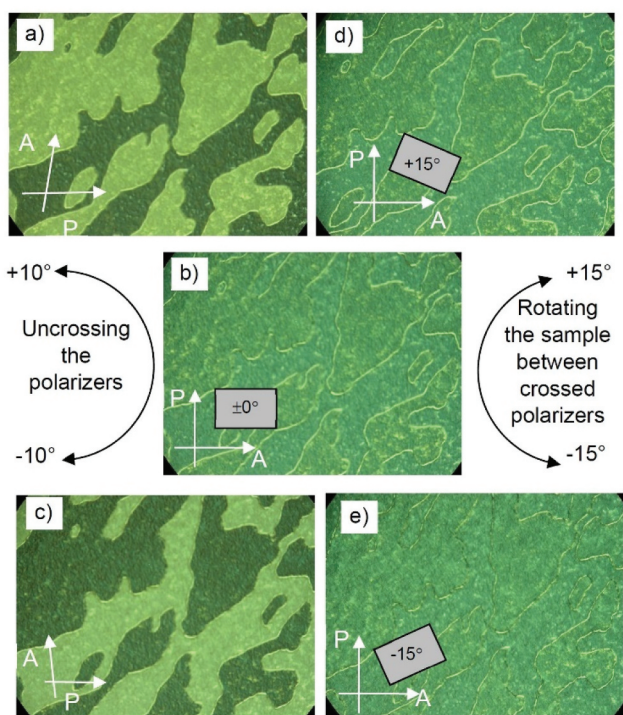


Figure 17. Textures of the $\text{SmC}_5^{[*]}$ phase of compound **AAF/O20** at $T = 130^\circ\text{C}$: (a,c) between slightly uncrossed polarizers, showing dark and bright domains, indicating the presence of areas with opposite chirality sense: (b) between crossed polarizers and (d, e) texture between crossed polarizers after rotation of the sample by 15° either clockwise or anticlockwise; the birefringence does not change which confirms chirality as origin of the effects seen in (a-c). Reprinted from ref. [101], copyright 2016, Wiley-VCH.

4.5. Surface supported mirror symmetry breaking by conglomerate formation in SmC_s phases ($\text{SmC}_s^{[*]}$ and $\text{SmC}_s\text{P}_R^{[*]}$)

A related conglomerate formation by surface supported mirror symmetry breaking is also found in the paraelectric SmC_s phases designated as $\text{SmC}_s^{[*]}$ and $\text{SmC}_s\text{P}_R^{[*]}$. Thin cells with homeotropic alignment show only a very small birefringence, in line with a helix developing between the two surfaces and perpendicular to the layer planes. Under slightly uncrossed polarizers dark and bright domains can be distinguished which invert their brightness by inverting the direction of the analyzer, whereas rotation of the sample between the polarizers does not change the texture, confirming a chiral conglomerate (Figure 17) [98–101]. The conglomerate texture is lost at the transition to the $\text{SmC}_s\text{P}_{AR}$ or SmC_sP_A phase with antipolar correlation, which are racemic. That these conglomerates cannot be observed in thick samples with reduced surface effects and in freely suspended films shows that this mirror symmetry breaking is surface supported, similar to that observed in the $\text{N}_{\text{CybC}}^{[*]}$ phases. However, its formation is more easily reproduced than in the $\text{N}^{[*]}$ phases. This is presumably a result of the enhanced cooperativity provided by the quasi infinite layers in comparison to the cybotactic clusters. Moreover, there is a relation between the appearance of a broad single peak in the current response curves and conglomerate formation. Whereas conglomerates are typically observed in the $\text{SmC}_s\text{P}_R^{[*]}$ phases showing a single broad current peak under the triangular wave electric field, they are only rarely found for paraelectric $\text{SmC}_s^{[*]}$ phases without detectable current peak. This means that also a growing coherence length of polar order has a stabilizing effect on conglomerate formation. This is in line with the suggested coupling between the emerging layer chirality and conformational molecular chirality [79,80].

4.6. Dark conglomerate formation

Notably, mirror symmetry broken isotropic dark conglomerate (DC) type LC sponge phases and related crystalline helical nanofilament phases (HNF, B4) [180,181] as known for highly bent BCLCs, weakly bent oxadiazoles [174,182] and some oligomesogens [183] are apparently missing in the series of 4-cyanoresorcinol based mesogens, even for compounds with silylated end-chains (see next Section) [19,184]. On the other hand, soft crystalline dark conglomerates (helical nano-crystallite phases, HNC) emerge and become dominating if the linear

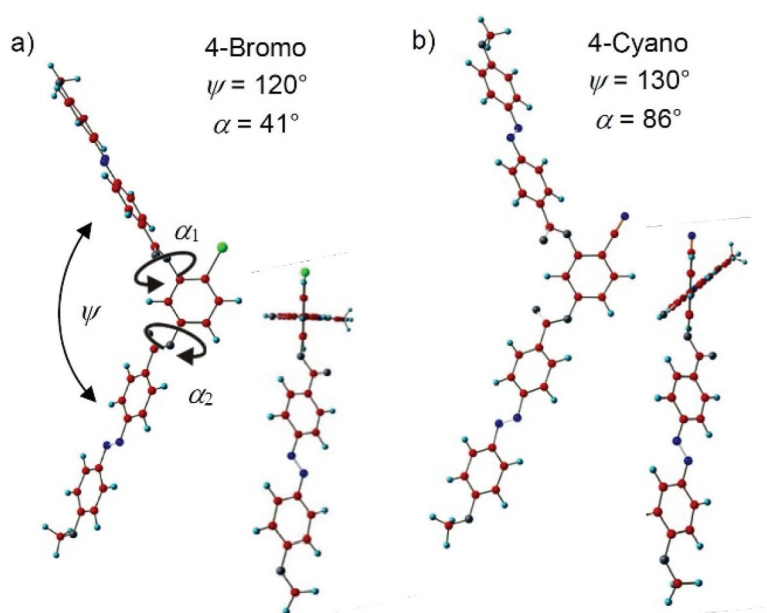


Figure 18. Energy minimum conformations obtained by DFT calculations for (a) the 4-bromo- and (b) 4-cyanoresorcinol based BCLCs with azobenzene wings; $\alpha = (90 - \alpha_1) + (90 - \alpha_2)$. Reprinted from ref. [188], copyright 2014, RSC.

4-CN group is replaced by bulky and more spherical 4-Br, 4-I or 4-CH₃ substituents in the azobenzene based BCLCs [185,186,187–190]. From DFT calculations it appears that the 4-CN group reduces the molecular bend (larger opening angle ψ), but induces a relatively large twist α between the π -planes of the wings ($\alpha = 86^\circ$, Figure 18) [188]. This obviously retains flat layers and supports the development of a heliconical twist between the layers by the twist between the alkyl end-chain orientations, thus supporting the formation of the heliconical phases, namely the short pitch $\text{Sm}(\text{CP})^{\text{hel}}$ phase and the surface stabilized long pitch heliconical states in the $\text{N}^{[*]}$ and $\text{SmC}_s(\text{P}_R)^{[*]}$ phases. However, this twist α obviously does not produce a sufficient transversal twist of the layers themselves, required for the formation of isotropic DC-type mesophases. This transversal twist obviously requires a stronger molecular bend, i.e. an opening angle ψ close to 120°. In addition, the bulkiness of the halogens and CH₃ provide significant layer distortion, destabilizing the layers and allowing an easier layer deformation.

4.7. The leaning phase and ferroelectricity by terminal chain silylation

Silylation of bent-core mesogens by using oligosiloxane or carbosilane groups at one alkyl chain end is known as the most efficient tool to stabilize ferroelectric switching smectic phases in achiral BCLCs [12, 19, 21–24, 191].

However, in most cases the developing SmC_sP_F phases escape from macroscopic polarization by layer modulation (B1 and B7 phases) [40] or formation of sponge-like dark conglomerate (DC) phases, and only after surface stabilization between glass surfaces ferroelectric states can be found in some cases [22]. However, for the terephthalate **TT/Si** (Figure 19) the birefringent SmC_sP_F phase is long time stable even as bulk material in the ground state and there is no relaxation to an antiferroelectric or DC phase, though the development of some layer modulation with short coherence length or long wave length (both being invisible in XRD) cannot fully be excluded. The formation of the $\text{SmC}_s\text{P}_{AR}$ and SmC_sP_A phases with antipolar order is in this case inhibited by the nano-segregated layers of the carbosilanes. These layers inhibit the fluctuations of the molecules between the layers and thus remove the entropic advantage of the antipolar packing (Figure 9(b), right) [19,21,192].

In contrast, the isomeric compound **BT/Si** differing only in the direction of one of the COO groups and combining only one terephthalate unit with a phenylbenzoate unit shows a weaker segregation, and the silyl group mainly acts as a bulky substituent reducing the coherence length of polar order. Therefore, the polar domain size in the SmA and SmC_s phases is only small, not showing a visible polarization peak, though there is mirror symmetry breaking by conglomerate formation in the $\text{SmC}_s^{[*]}$ phase. **BT/Si** also tends to assume synpolar order in the layers, but surprisingly, the tilt direction coincides with the polar direction in this ferroelectric smectic phase,

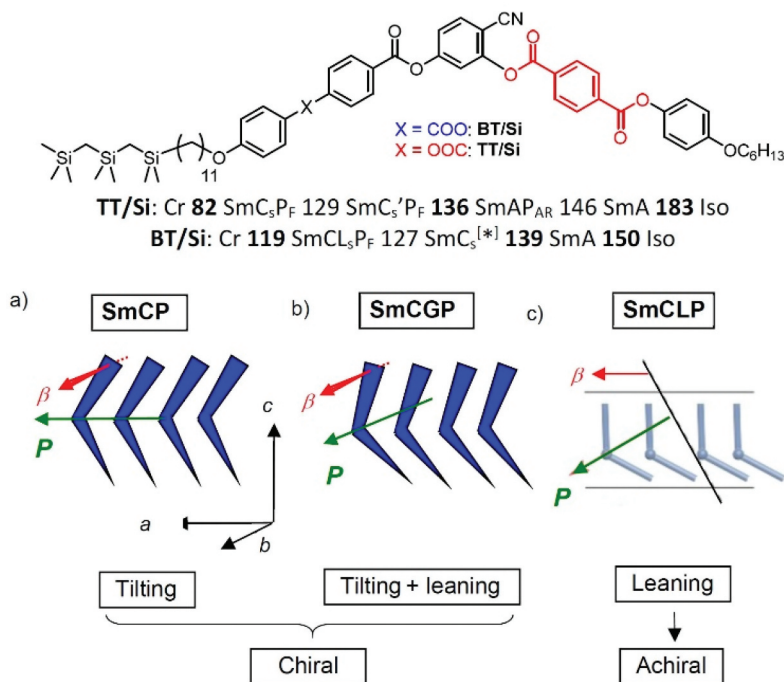


Figure 19. Formula and phase transitions ($T/^\circ\text{C}$) of the silylated compounds **TT/Si** and **BT/Si** and the structures of the different types of tilted phases of bent-core molecules [184].

providing the first case of a so-called leaning phase SmCL_sP_F (Figure 19(c)) [184,193]. This is a new type of polar smectic C phase complementing the previously known SmC_sP_F phase with orthogonal directions of tilt and polar order and the SmC_GP_{A/F} phases [194–196] with inclined directions of tilt/polar directions by the new syn-leaning SmCL_sP_F phase with coincidence of tilt and polar directions (Figure 19).

Due to the coincidence of polar and tilt directions, the leaning phases are achiral [197]. It is remarkable that achiral phases, SmA^{LT}P_F for compounds **TT/n** and SmCL_sP_F for **BT/Si**, are formed at relatively low temperature though the packing becomes denser and synchronization of molecular conformations is likely to become more important for self-assembly. A possible explanation for the transition from the usually observed polar SmC phases of bent-core molecules, with chiral layers (due to the orthogonal combination of polar direction and tilt direction) to the achiral SmA^{LT}P_F and SmCL_sP_F phases could be that the enantiophilic self-assembly (racemate formation) becomes advantageous over the enantiophobic (conglomerate formation), as explained in Section 4.3. Due to the bulky silyl groups **BT/Si** has a stronger tendency to retain tilt than the non-silylated compounds of series **BT/n** and **TT/n**. Their tilt cannot be removed, and therefore removal of the inclination between tilt and polar direction by formation of the leaning SmCL_sP_F phase becomes the preferred alternative.

4.8. Effects of branched chains

Branched chains reduce the packing density of the bent aromatic rods, i. e. phase transitions as well as SmC_sP_F domain formation and their growth and fusion to polar layers are shifted to lower temperatures. It also appears, that due to the reduced packing density even the polar smectic phases do not represent classical B2 phases with quasi infinite polar order in the layers, but the layers still retain a significant polar domain structure which is indicated by the apostrophe in the phase abbreviations (SmC_{s'}P_A). Figure 20(a) shows the temperature dependent development of the layer spacing in the smectic phases of compound *rac*-**TT/Ocit** with two branched 3,7-dimethyloctyloxy end-chains derived from *rac*-citronellol (black squares) [198]. The decrease of the layer spacing d in the uniaxial SmA range between 110 and 95°C can be attributed to the emergence and growth of a random tilt due to the growth of SmC_sP_F domains and therefore at least this range of the uniaxial SmA phase can be considered as a de Vries like tilted smectic phase. The polar domain structure is retained in the biaxial SmC phase. That the phase is biaxial though no optical tilt can be identified in the absence of an applied E-field (Figure 20(b), red) means that the synpolar and synclinc alignment of the SmC_sP_F domains becomes on average antipolar and anticlinic and in this respect this

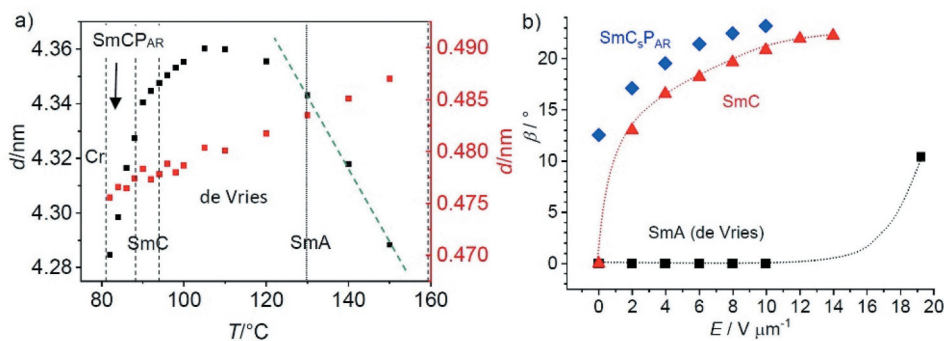


Figure 20. (a) Temperature dependence of the d -value of the small angle (black) and the maxima of the diffuse wide-angle scattering (red) in the paraelectric mesophases of *rac*-**TT/Ocit** (under these conditions crystallization takes place before the transition to the polar phase); (b) field strength dependence of the optical tilt angle β of *rac*-**TT/Ocit** in the paraelectric smectic phases. Reprinted from ref. [198], copyright 2016, RSC.

phase can be considered as a de Vries like SmA_b phase [198]. Application of a small E-field induces a significant tilt due to the alignment of the SmC_sP_F domains. This field induced tilt by domain alignment can be considered as a non-classical electroclinic effect which is also observed in the de Vries SmA phase range, where it requires larger E-fields (Figure 20(b), black).

It is noted that, in addition, the branching of the molecules contributes to the stabilization of the ferroelectric order due to the layer decoupling effect of the bulkier and more disordered branched chains [199,200]. Moreover, chain branching can create stereogenic centers leading to permanent molecular chirality which can be uniform or racemic.

5. Effects of permanent molecular chirality

5.1. Non-classical electroclinic effect and switching modes

Permanent molecular chirality is known to reduce the phase symmetry of tilted smectic phases and thus was found to induce ferroelectric switching in SmC_s and antiferroelectric switching in SmC_a phases of rod-like molecules [130,131]. Alternatively, the reduction of phase symmetry is achieved by the polar order developing in the layers of the smectic phases of bent-core molecules, which thus become chiral and show ferroelectric or antiferroelectric switching, in this case independent on the mode of tilt correlation. The effects of the permanent molecular chirality on the mesophases of weakly bent mesogens was studied by comparing the enantiomeric pure compound (*S*)-**TT/Ocit** with its racemate *rac*-**TT/Ocit** [198]. In the de Vries SmA^* range of

(*S*)-**TT/Ocit** (Table 2) there is a significant electroclinic effect already at low field strength (Figure 21 (a)), meaning that the chiral SmC_sP_F domains with one specific sense of chirality are stabilized by the diastereomeric coupling with the permanent molecular chirality, thus supporting uniform polar order (Figure 21(a)). As a result of this diastereomeric coupling the double current peak in the $\text{SmC}_s\text{P}_{AR}$ range of the racemate is replaced by a single peak in the SmC_sP_R^* range of the enantiomer. Moreover, it changes the switching from a superparaelectric-like switching in the SmC_sP_A range of the racemate to ferroelectric in the corresponding SmC_sP_F^* phase range of the enantiomer (Figure 21(b,c)) [198]. This means, that for weakly bent BCLC the synpolar order is supported by the molecular chirality, whereas for more strongly bent molecules the spatially induced polar order (polar packing of the bend directions) becomes dominating, which usually prefers antiferroelectric phases even in the presence of molecular chirality and if the tilt is synclinic [198].

Interestingly, between 73 and 81°C, in the *achiral* SmC_sP_A phase range of *rac*-**TT/Ocit** (Table 2), the switching takes place by collective rotation around the long axis as typical for the non-helical LC phases of the 4-cyanoresorcinols, whereas the corresponding *chiral* SmC_sP_F^* phase of the (*S*)-enantiomer switches by collective precession on a cone which retains the layer chirality [198]. Thus, the effect of permanent molecular chirality is the same as that of the spontaneously broken symmetry in the $\text{Sm}(\text{CP})^{\text{hel}}$ phase of the related achiral compounds **TT/n** with linear alkyl chains (see section 4.1). This indicates a significant diastereomeric coupling between molecular and helical chirality on the one hand, and the layer chirality on the other hand, i.e. the energetically favored

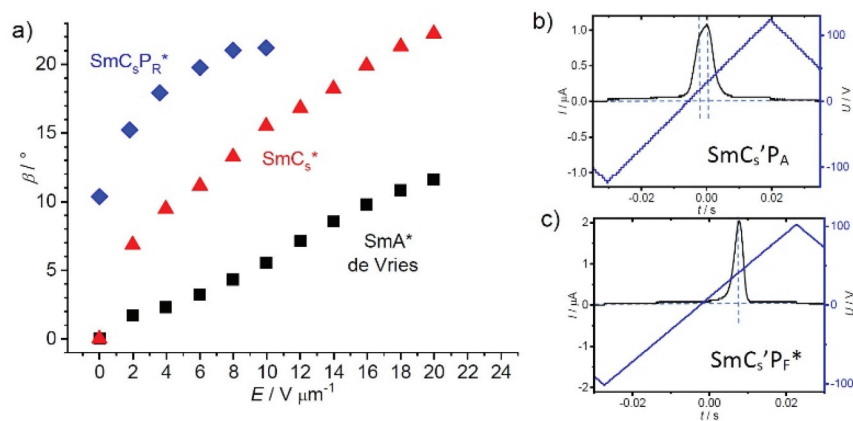


Figure 21. (a) Field strength dependence of the optical tilt of (*S*)-**TT/Ocit** in the distinct paraelectric smectic phases and; b,c) switching current response curves in the polar smectic phases of racemate and enantiomer at the same temperature (75°C); the (anti) ferroelectric character of switching in (b) is additionally confirmed by electrooptical investigations. The slope of the $\beta = f(E)$ curve in the SmC^* phase of (*S*)-**TT/Ocit** is smaller than in the SmC phase of the racemate *rac*-**TT/Ocit** (compare Figures 20(a) and 21(a)) due to helix unwinding. Reprinted from ref. [198], copyright 2016, RSC.

couple between molecular/helical and layer chirality has to be retained during the switching process. However, below 73°C, after transition to the anticlinic phase, the switching takes place by precession on a cone for both, the racemate ($SmC_a'P_A$) and the (*S*)-enantiomer ($SmC_a'P_A^*$), meaning that the bent molecular shape becomes dominating and molecular chirality is no more required for inhibition of the rotation around the long axis. Thus, in the $SmC_a'P_A^{(*)}$ phase of the compounds with branched chains the switching takes place by precession on a cone, whereas in the SmC_aP_A phase of the related achiral compounds **TT/n** with linear alkyl chains the molecules rotate collectively around the long axis. This is remarkable, because the opposite would be expected, i.e. the branched chains are expected to lead to a reduced packing density of the cores and therefore should support the rotation around the long axis (planar alignment in both cases). A possible explanation could be that a local segregation of the enantiomers takes place, which leads to a kind of nanoscale conglomerate and this local chirality provides an energetic penalty for the transition to an achiral phase structure, thus disfavoring the rotation around the long axis.

5.2. Diastereomerism between superstructural and permanent molecular chirality

In contrast, in the SmC_sP_A phase of the biphenyl compound **PP/Ocit** with a shorter bent core unit the switching takes place by collective rotation around the long axis for the racemate as well as for

the (*S*)-enantiomer (Figure 22), indicating a weaker coupling between molecular and superstructural chirality [90]. Under an applied DC voltage a highly birefringent uniformly chiral $SmC_sP_F^*$ state is induced from the $SmC_sP_A^*$ ground state of (*S*)-**PP/Ocit** (Figure 21(a, c)) by rotation around the long axis. This field-induced SmC_sP_F state has uniform (+)- or (-)-layer chirality, depending on the direction of the applied electric field. While the field induced (+)- SmC_sP_F state (Figure 22(a)) is long time stable, the field induced (-)- SmC_sP_F state (Figure 22(c)) is instable for (*S*)-**PP/Ocit** and slowly relaxes within about one minute to the more stable diastereomeric (+)- SmC_sP_F -(*S*)-**PP/Ocit** state by slow reorganization of the molecules with reversal of the tilt direction, while the polar director is fixed by the applied E-field (Figure 22(d-f)) [201]. This causes the change of the direction of the optic axis that now nearly coincides with the direction of the polarizer, leading to an almost dark texture (Figure 22(f)). Upon inverting the direction of the applied field, the molecules flip around the molecular long axis to another dark state (Figure 22(h)). As the switching takes place around the long axis the orientation of the optical axis is not changed. Therefore, the texture remains dark, but the polar direction, and hence, the layer chirality is inverted (Figure 22(k)), i.e. the structure is flipped back to the instable (-)- SmC_sP_F -(*S*)-**PP/Ocit** state (Figure 22(h)) and this slowly transforms to the stable (+)- SmC_sP_F -(*S*)-**PP/Ocit** state by tilt-flipping (Figure 22(h-j)). This experiment confirms the coupling between the fixed molecular chirality and the field dependent superstructural layer chirality,

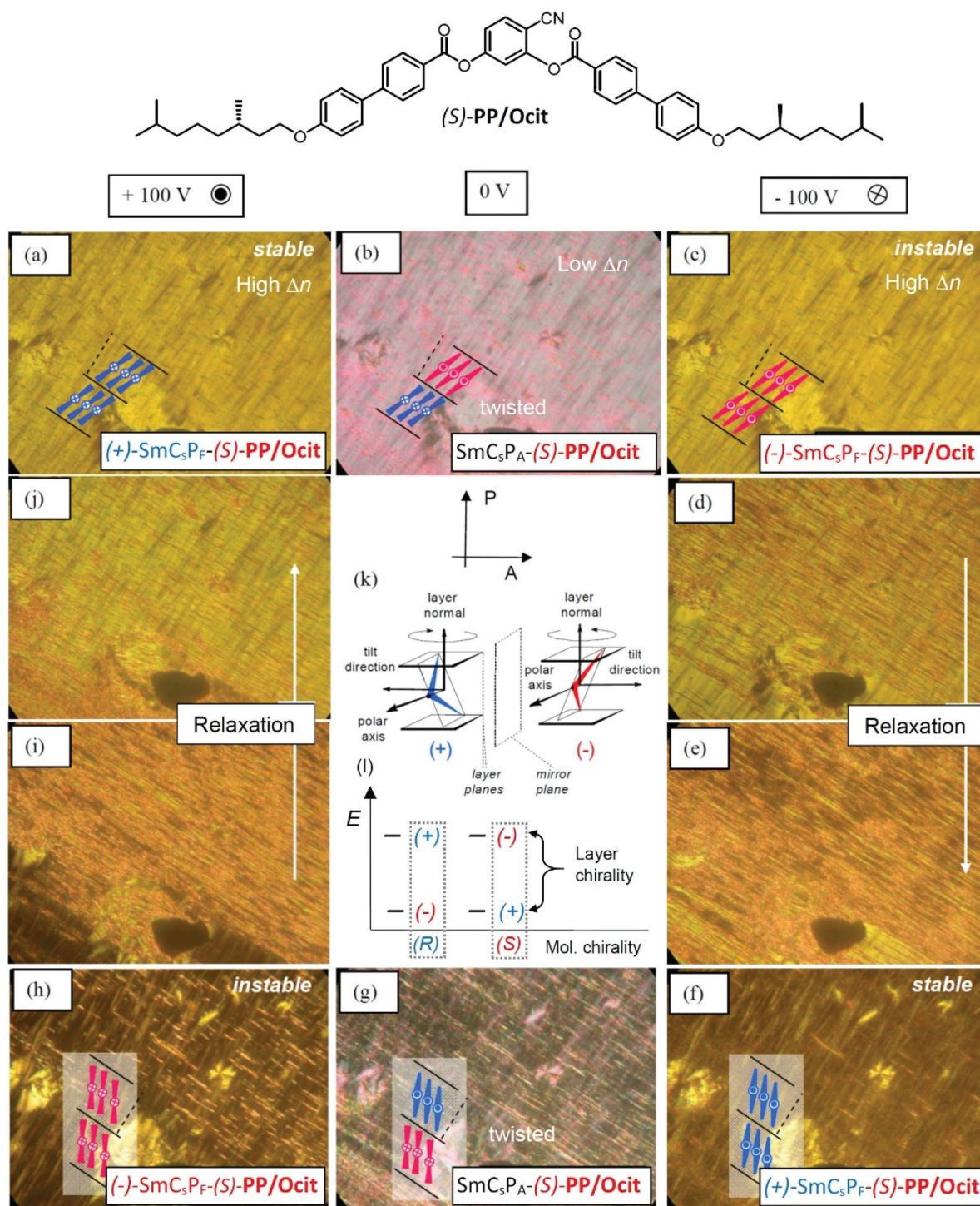


Figure 22. Textures as observed for the SmC_sP_A^* phase of compound $(S)\text{-PP/Ocit}$ under an applied DC field at $T = 43^\circ\text{C}$; in a $6\ \mu\text{m}$ polyimide coated ITO cell with planar alignment; (c) and (h) were taken immediately after field reversal, whereas (d-f) and (i, j) were taken with a time difference of 20 s between each photo; it is noted that the birefringence at 0 V in (b) and (g) is much *lower* than under the applied field (see SI for a T -dependence of Δn). (k) shows the origin of layer chirality [112] and (l) shows the energy diagram of the diastereomeric coupling between molecular chirality and layer chirality. Reprinted with modifications from ref. [90], copyright 2016, RSC.

leading to energetically distinct diastereomeric states (Figure 22(l)). It is noted that the 0 V states have a much (almost one order) lower birefringence than

the field induced states due to a reduced order parameter arising either from a tilt randomization or an emerging helical twist developing after removal of

the alignment field (Figure 22(b, g)). That the 0 V state indeed has lowest birefringence is obvious from the sequence of textures depending on the applied voltage shown in Fig. S3 in the Supporting information.

5.3. Giant magnetic field effects

Another interesting and unprecedented chirality effect was observed in the smectic phases of **BB/12-cit** having only one branched chiral chain and an achiral linear chain at the opposite end (Figure 23) [202]. For this compound huge magnetic field effects on the layer spacing were found with an opposite effect of the magnetic field on racemate and pure enantiomer. Whereas a layer expansion by 0.2–0.4 nm is observed for the racemate (Figure 23(c)), a layer shrinkage by up to 0.6 nm is found for the enantiomer under an applied magnetic field of only one Tesla (Figure 23(d)). This is explained as an effect of the magnetic field on the core order parameter. In the racemate the field induced increase of the orientational order parameter leads to a denser core packing; this increases the alkyl chain order and decreases the possibility of chain intercalation which in turns rises the layer spacing (Figure 23(a)). For the enantiomeric pure compound, the helicoidal (longitudinal) twist allows an optimized packing of the transiently helical molecules with a preferred helix sense due to the coupling of permanent molecular and transient

conformational chirality. This means that already without applied magnetic field the chains are in the most stretched conformation and the layer spacing at 90°C corresponds to that observed for the racemate under the magnetic field [202]. It is known that the magnetic field has a stronger suppressing effect on the longitudinal than on the transversal twist and this at first removes the helicoidal (longitudinal) twist [203,204]. Because the chirality of the molecules is permanent, conformational helicity has to be preserved. Therefore, the longitudinal twist cannot simply be removed, but it is replaced by a developing transversal twist within the layers. This transversal twist distorts the layers, reduces the order parameter and hence the packing density. This provides more space between the alkyl chains for chain folding or intercalation, thus reducing the layer spacing under the applied magnetic field (Figure 23(b)) [202].

It appears that this strong magnetic effect is related to the non-symmetric molecular structure of the molecule having one branched and one linear chain, which provides just the right chain volume for a transition between intercalated and non-intercalated smectic phases.

A related TT-based compound with one chiral lactate side chain was recently reported to show a ferroelectric-like switching in a uniaxial smectic phase, but no comparison with the racemate was made in this case [205].

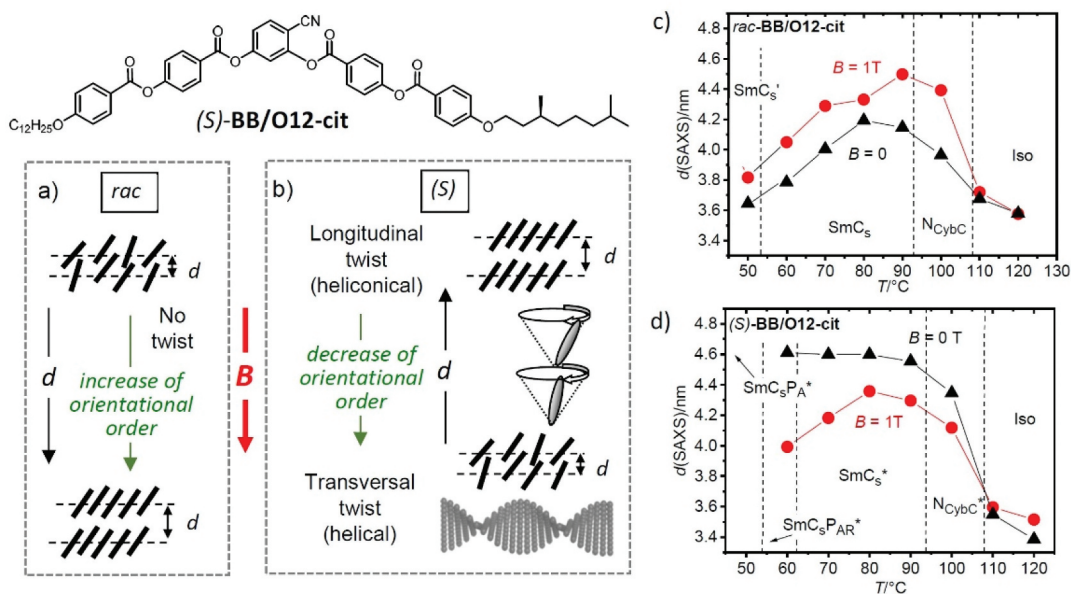
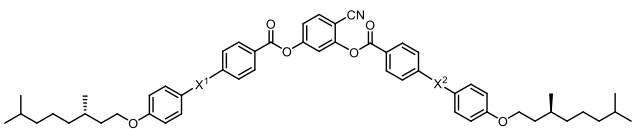


Figure 23. (a,b) Effects of the magnetic field on the orientational order parameter and layer distance of the racemic and uniformly chiral compound **BB/O12-cit**; (c,d) show the d -values of the SAXS depending on temperature and magnetic field [202].

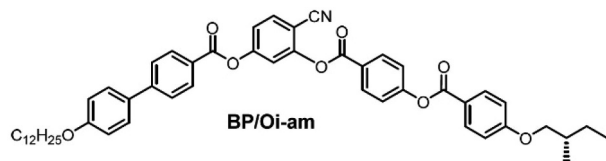
Table 2. Mesophases and phase transition temperatures of the branched chiral compounds with (*S*)-configuration and their racemic mixtures (*rac*) [90,198].^a


Compd.	X ¹	X ²	Phase transitions T/°C
<i>rac</i> -BB/Ocit	COO	OOC	Cr 84 N _{Cybc} 60 Iso
(<i>S</i>)-BB/Ocit	COO	OOC	Cr 80 (Mx 42) BPIII 58 Iso
<i>rac</i> -PP/Ocit	-	-	Cr 91 (SmC _s P _A 50 SmC _s 74) SmA 99 Iso
(<i>S</i>)-PP/Ocit	-	-	Cr 85 (SmC _s P _A * 50 SmC _s * 73) SmA* 99 Iso
<i>rac</i> -TT/Ocit	OOC	COO	Cr 98 (SmC _a 'P _A 73 SmC _s 'P _A 81 SmC _s P _{AR} 87 SmC 93) de Vries SmA/SmA 159 Iso
(<i>S</i>)-TT/Ocit	OOC	COO	Cr 106 (SmC _a 'P _A * 73 SmC _s 'P _F * 81 SmC _s P _R * 87 SmC* 93) de Vries SmA*/SmA* 159 Iso

^aAbbreviations: in SmC_a'P_A and SmC_s'P_A the apostrophe indicates the polar domain structure of these phases; for SmC no layer correlation (*syn/anti*) is given because there is anticlinic correlation between the synclinic domains.

5.4. Helical superstructure and chirality frustrated LC phases

Besides the above-mentioned chirality effects, the molecular chirality affects the phase structure in the usual way by introducing helical twist. In contrast to rod-like molecules where strong chirality is required to obtain new chirality modulated phases, for the bent molecules even stereogenic centers having a weak helical twisting power are sufficient to induce highly frustrated LC phases. For example, compound (*S*)-**BB/Ocit** shows a broad BPIII phase (blue fog phase) with unusually large Kerr constants (Table 2) [90,206]. Different types of blue phases were also induced in the nematic phases of achiral 4-cyanoresorcinols by addition of chiral dopants, and in nematic/cholesteric phases of rod-like molecules by adding 4-cyanoresorcinol derived BCLCs, indicating their amplification effect on helicity [207–209]. This is also evidenced by the formation of the highly frustrated Twist Grain Boundary phases (TGBA and TGBC) by the 4-cyanoresorcinol **BP/Oi-am** with a weakly chiral **isoamyl** group at only one end [210]. This indicates the much stronger effects of permanent molecular and transient conformational chirality on the self-assembly of BCLCs compared to linear mesogens.



rac-**BP/Oi-am**: Cr 95 (SmC^[*] 88) SmA 96 N_{CyBA} 108 °C Iso
(*S*)-**BP/i-am**: Cr 98 (SmC*/TGBC 88) TGBA 96 N*_{CyBA} 108 °C Iso

It is noted here, that the first example of TGB phases of bent-core mesogens [211] was observed by Sadashiva et al. and he was also involved in the report about induction of BPIII phases by addition of bent-core mesogens to cholesteric phases of rod-like molecules [212], once again showing his seminal contributions to different aspects of LC research.

6. Hockey-stick molecules, dimesogens and oligomesogens

Besides the bent-core molecules with two polyaromatic wings of almost identical length also related hockey stick molecules, having a different length of the wings have been reported [213]. Moreover, some end-connected homo- and heterodimers [214,215] as well as different types of laterally connected heterodimers combining 4-cyanoresorcinol based BCLCs with rod-like mesogens have been described [216]. It is noted that some dimesogens (e.g. **Di3**) can show especially broad regions of the cybotactic nematic phase [215]. Three selected examples of dimesogens are shown in Figure 24, among them compound **Di3** combining the 4-cyanoresorcinol core with a 4-cyanobiphenyl (CB) unit. It is noted that the CB unit was also combined with other bent cores leading to broad cybotactic nematic phase regions [217,218] eventually involving the N_{TB} phase [218]. However, polymeric, dendrimeric and other larger molecular structure involving the 4-cyanoresorcinol unit have not been investigated so far.

7. Summary

The current state of knowledge of the LC self-assembly of 4-cyanoresorcinol based BCLC is reviewed. The 4-cyano group at the central 1,3-substituted benzene

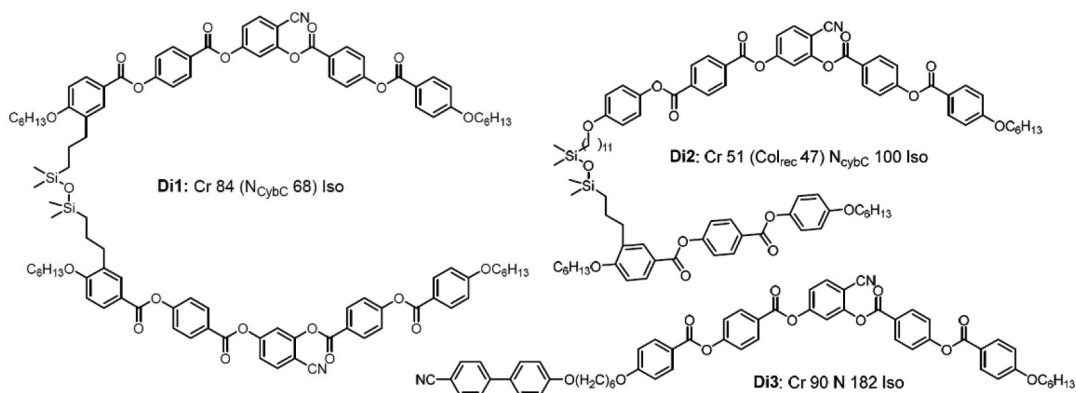


Figure 24. Selected examples of 4-cyanoresorcinol based mesogenic dimers ($T/^\circ\text{C}$).

ring of bent-core molecules causes a reduced molecular bend and thus provides compounds at the cross-over between classical rod-like and typical bent-core mesogens. This gives rise to at least five new LC phase structures (SmC_sP_R , $\text{SmC}_s\text{P}_{AR}$, $\text{SmA}^{\text{LT}}\text{P}_F$, SmCL_sP_F , $\text{Sm}(\text{CP})^{\text{hel}}$). The CN group also supports the formation of cybotactic nematic phases (N_{Cybc} , N_{CybA}). Lowering the temperature or lengthening the terminal alkyl chains leads to an almost continuous transition between these nematic and smectic phases by the growth of the cybotactic SmC clusters. Within the smectic phases, a continuous transition takes place from the apolar de Vries-like SmA and the SmC_s phases via paraelectric and superparaelectric ranges (SmAP_R , $\text{SmC}_s\text{P}_R^{[*]}$, SmAP_{AR} , $\text{SmC}_s\text{P}_{AR}$) and finally to polar smectic phases (SmC_sP_A , SmC_aP_A) by the growth of polar SmC_sP_F domains. As the polar order becomes long-range, a series of new LC phases emerges just before the transition to the antiferroelectric phases. Among them, modulated smectic phases (M1 , $\text{Sm}\tilde{\text{C}}_s\text{P}_A$) for compounds had a strong tendency to form tilted phases and a new heliconical smectic phase ($\text{Sm}(\text{CP})^{\text{hel}}$) if there is reduced tilt. The heliconical phase occurs at the SmC_aP_A – SmC_sP_A transition and either replaces the chiral SmC_aP_A phase as ground state structure or the racemic SmC_sP_A phase as an E-field induced long-time stable phase. It is considered as analogous to the SmC_α^* phase found for permanently chiral rod-like molecules.

It is also shown that diastereomerism arising between the molecular chirality and the superstructural helical and layer chiralities has a significant influence on the mesophase structures and the switching behavior. It is postulated that the change from enantiophobic (conglomerate forming) to enantiophilic (racemate forming) self-assembly contributes to the unusual transition from the tilted polar smectic phases with intrinsic layer

chirality to alternative achiral polar phases, either being non-tilted ($\text{SmA}^{\text{LT}}\text{P}_F$) or assuming a leaning-type tilt (SmCL_sP_F).

The heliconical $\text{Sm}(\text{CP})^{\text{hel}}$ phase is of practical interest for fast switching electro-optical devices, either using the in-plane switching of the secondary optical axis or the V-shaped grey scale switching by helix deformation. A local helical organization is even retained in the adjacent SmC_aP_A phase, which also shows a fast switching of the secondary optical axis. The ferroelectric switching in the non-tilted $\text{SmA}^{\text{LT}}\text{P}_F$ and the leaning phase and the strong electroclinic and magnetic field effects of the permanently chiral 4-cyanoresorcinols provide additional applications.

Overall, 4-cyanoresorcinol based BCLC represent a unique class of compounds providing a variety of new phenomena, phase structures, effects and applications and thus improve our basic understanding of complex self-assembly in LC and other soft matter systems.

Acknowledgments

The work reviewed in this manuscript is the result of several Master's and PhD students (C. Keith, A. Lehmann, E. Westphal, M. Poppe), postdocs (S. Poppe, M. Prehm) and guest researchers (M. Alaasar, G. Shanker) over the recent decade working at Halle University and the collaboration with numerous scientists and their groups from different other places (N. Clark, Boulder; M.K. Das, Siliguri; A. Eremin, Magdeburg; J. Lagerwall, Luxemburg; F. Liu, Xi'an; H. Ocak and B. Bilgin-Eran, Istanbul and J. K. Vij, Dublin). Special thanks to M. Alaasar and H. Ocak, who designed and synthesized the azobenzene-based and chiral BCLCs, respectively, and to J. K. Vij who has supervised most of the electrooptical investigations and switching experiments. The authors work in this area has been supported by the EU with the FP7 funded collaborative project

BIND (216025) and the Deutsche Forschungsgemeinschaft (Ts 39/24-1/2).

Disclosure statement

No potential conflict of interest was reported by the author(s).

Funding

This work was supported by the Deutsche Forschungsgemeinschaft [Ts 39/24]; Seventh Framework Programme [216025].

References

- [1] Chandrasekhar S, Sadashiva BK, Suresh KA. Liquid crystals of disc-like molecules. *Pramana*. 1977;9:471–480.
- [2] Madhusudana NV, Sadashiva BK, Moodithaya KPL. Re-entrant nematic phase in pure compound at atmospheric pressure. *Curr Sci*. 1979;48:613–614.
- [3] Chandrasekhar S, Ratna BR, Sadashiva BK, et al. A thermotropic biaxial nematic liquid crystal. *Mol Cryst Liq Cryst*. 1988;165:123–130.
- [4] Chandrasekhar S, Sadashiva BK, Srikanta BS. Paramagnetic nematic liquid crystals. *Mol Cryst Liq Cryst*. 1987;15:93–107.
- [5] Reddy RA, Sadashiva BK. Influence of fluorine substituent on the mesomorphic properties of five-ring ester banana-shaped molecules. *Liq Cryst*. 2003;30:1031–1050.
- [6] Reddy RA, Raghunathan VA, Sadashiva BK. Novel ferroelectric and antiferroelectric smectic and columnar mesophases in fluorinated symmetrical bent-core compounds. *Chem Mater*. 2005;17:274–283.
- [7] Reddy RA, Sadashiva BK. New phase sequences in banana-shaped mesogens: influence of fluorine substituent in compounds derived from 2,7-dihydroxynaphthalene. *J Mater Chem*. 2004;14:1936–1947.
- [8] Reddy RA, Sadashiva BK. Direct transition from a nematic phase to a polar biaxial smectic A phase in a homologous series of unsymmetrically substituted bent-core compounds. *J Mater Chem*. 2004;14:310–319.
- [9] Reddy RA, Sadashiva BK, Pratibha R, et al. Biaxial smectic A phase in homologous series of compounds composed of highly polar unsymmetrically substituted bent-core molecules. *J Mater Chem*. 2002;12:943–950.
- [10] Murthy HNS, Sadashiva BK. A polar biaxial smectic A phase in new unsymmetrical compounds composed of bent-core molecules. *Liq Cryst*. 2004;31:567–578.
- [11] Guo L, Dhara S, Sadashiva BK, et al. Polar switching in the smectic-AdPA phase composed of asymmetric bent-core molecules. *Phys Rev E*. 2010;81:011703.
- [12] Dantlgraber G, Eremin A, Diele S, et al. Chirality and macroscopic polar order in a ferroelectric smectic liquid crystalline phase formed by achiral polyphilic bent-core molecules. *Angew Chem Int Ed*. 2002;41:2408–2412.
- [13] Amaranatha RA, Sadashiva BK. Ferroelectric properties exhibited by mesophases of compounds composed of achiral banana-shaped molecules. *J Mater Chem*. 2002;12:2627–2632.
- [14] Pratibha R, Madhusudana NV, Sadashiva BK. An orientational transition of bent-core molecules in an anisotropic matrix. *Science*. 2000;288:2184–2187.
- [15] Hegmann T, Kain J, Diele S, et al. Evidence for the existence of the mcmillan phase in a binary system of a metallomesogen and 2,4,7-Trinitrofluorenone. *Angew Chem Int Ed*. 2001;40:887–890.
- [16] Gray GW, Harrison KJ, Nash JA. New family of nematic liquid crystals for displays. *Electron Lett*. 1973;9:130–131.
- [17] Sadashiva BK, Reddy RA, Pratibha R, et al. Biaxial smectic A liquid crystal in a pure compound. *Chem Commun*. 2001;2140–2141.
- [18] Sadashiva BK, Reddy RA, Pratibha R, et al. Biaxial smectic A phase in homologous series of compounds composed of highly polar unsymmetrically substituted bent-core molecules. *J Mater Chem*. 2002;12:943–950.
- [19] Keith C, Reddy RA, Hauser A, et al. Silicon-containing polyphilic bent-core molecules: the importance of nano-segregation for the development of chirality and polar order in liquid crystalline phases formed by achiral molecules. *J Am Chem Soc*. 2006;126:3051–3066.
- [20] Keith C, Reddy RA, Tschierske C. The first example of a liquid crystalline side-chain polymer with bent-core mesogenic units: ferroelectric switching and spontaneous achiral symmetry breaking in an achiral polymer. *Chem Commun*. 2005;871–873.
- [21] Keith C, Reddy RA, Hahn H, et al. The carbosilane unit as a stable building block for liquid crystal design: a new class of ferroelectric switching banana-shaped mesogens. *Chem Commun*. 2004;1898–1899.
- [22] Reddy RA, Tschierske C. Bent-core liquid crystals: polar order, superstructural chirality and spontaneous desymmetrisation in soft matter systems. *J Mater Chem*. 2006;16:907–961.
- [23] Zhang Y, Baumeister U, Tschierske C, et al. Achiral bent-core molecules with a series of linear or branched carbosilane termini: dark conglomerate phases, supra-molecular chirality and macroscopic polar order. *Chem Mater*. 2010;22:2869–2884.
- [24] Reddy RA, Zhu C, Shao R, et al. Spontaneous ferroelectric order in a bent-core smectic liquid crystal of fluid orthorhombic layers. *Science*. 2011;332:72–77.
- [25] Meyer RB. Structural problems in liquid crystal physics, molecular fluids. In: Balian RG, and Weil Geditors. *Les houches summer school in theoretical physics*. New York (NY): Gordon and Breach; 1976. p. 271–343.
- [26] Dozov I. On the spontaneous symmetry breaking in the mesophases of achiral banana-shaped molecules. *Europhys Lett*. 2001;56:247–253.
- [27] Panov VP, Nagaraj M, Vij JK, et al. Spontaneous periodic deformations in nonchiral planar aligned bimesogens with a nematic-nematic transition and a negative elastic constant. *Phys Rev Lett*. 2010;105:167801.

- [28] Cestari M, Diez-Berart S, Dunmur DA, et al. Phase behavior and properties of the liquid-crystal dimer 1',7''-bis (4-cyanobiphenyl-4'-yl) heptane: a twist-Bend nematic liquid crystal. *Phys Rev E*. 2011;84:031704.
- [29] Henderson PA, Imrie CT. Methylene-linked liquid crystal dimers and the twist-Bend nematic phase. *Liq Cryst*. 2011;38:1407–1414.
- [30] Borshch V, Kim YK, Xiang J, et al. Nematic twist-Bend phase with nanoscale modulation of molecular orientation. *Nat Commun*. 2013;4:2635.
- [31] Chen D, Porada JH, Hooper JB, et al. Chiral heliconical ground state of nanoscale pitch in a nematic liquid crystal of achiral molecular dimers. *Proc Natl Acad Sci USA*. 2013;110:15931–15936.
- [32] Mandle RJ, Davis EJ, Archbold CT, et al. Microscopy studies of the nematic NTB phase of 1,11-di-(100-cyanobiphenyl-4-yl)undecane. *J Mater Chem C*. 2014;2:556–566.
- [33] Paterson DA, Abberley JP, Harrison WTA, et al. Cyanobiphenyl-based liquid crystal dimers and the twist-Bend nematic phase. *Liq Cryst*. 2017;44:127–146.
- [34] Mandle RJ, Goodby JW. Molecular flexibility and bend in semi-rigid liquid crystals: implications for the heliconical nematic ground state. *Chem Eur J*. 2019;25:14454–14459.
- [35] Mandle JM. The dependency of twist-Bend nematic liquid crystals on molecular structure: a progression from dimers to trimers, oligomers and polymers. *Soft Matter*. 2016;12:7883–7901.
- [36] Reddy RA, Sadashiva BK. Helical superstructures in the mesophase of compounds derived from 2-cyanoresorcinol. *Liq Cryst*. 2002;29:1365–1367.
- [37] Murthy HNS, Sadashiva BK. Banana-shaped mesogens: a new homologous series of compounds exhibiting the B7 mesophase. *Liq Cryst*. 2003;30:1051–1055.
- [38] Reddy RA, Sadashiva BK. Unusual mesomorphic behaviour in bent-core compounds derived from 5-cyanoresorcinol. *Liq Cryst*. 2004;31:1069–1081.
- [39] Pelzl G, Diele S, Jakli A, et al. Helical superstructures in a novel smectic mesophase formed by achiral banana-shaped molecules. *Liq Cryst*. 2006;33:1519–1523.
- [40] Coleman DA, Fernsler J, Chattham N, et al. Polarization-modulated smectic liquid crystal phases. *Science*. 2003;301:1204–1211.
- [41] Weissflog W, Kovalenko L, Wirth I, et al. SmA–SmC–B2 polymorphism in an achiral cyano substituted banana-shaped mesogen. *Liq Cryst*. 2000;27:677–681.
- [42] Dunemann U, Schröder MW, Reddy RA, et al. The influence of lateral substituents on the mesophase behaviour of bananashaped mesogens. Part II. *J Mater Chem*. 2005;15:4051–4061.
- [43] Kovalenko L, Schröder MW, Reddy RA, et al. Unusual mesomorphic behaviour of new bent-core mesogens derived from 4-cyanoresorcinol. *Liq Cryst*. 2005;32:857–865.
- [44] Pelzl G, Weissflog W. Mesophase behaviour at the borderline between calamitic and banana-shaped mesogens. In: Ramamoorthy A, editor. *Thermotropic Liquid Crystals: Recent Advances*. The Netherlands: Springer; 2007. p. 1–58.
- [45] Weissflog W, Murthy HNS, Diele S, et al. Relationships between molecular structure and physical properties in bent-core mesogens. *Phil Trans Royal Soc A*. 2006;364:2657–2679.
- [46] Eremin A, Diele S, Pelzl G, et al. Experimental evidence for an achiral orthogonal biaxial smectic phase without in-plane order exhibiting antiferroelectric switching behavior. *Phys Rev E*. 2001;64:051707.
- [47] Pan L, McCoy BK, Wang S, et al. Surface and bulk uniaxial to biaxial smectic-A transition in a bent core liquid crystal. *Phys Rev Lett*. 2010;105:117802.
- [48] Pocięcha D, Gorecka E, Čepič M, et al. Polar order and tilt in achiral smectic phases. *Phys Rev E*. 2006;74:021702.
- [49] Keith C, Lehmann A, Baumeister U, et al. Nematic phases of bent-core mesogens. *Soft Matter*. 2010;6:1704–1721.
- [50] Pelzl G, Diele S, Weissflog W. Banana-shaped compounds-A new field of liquid crystals. *Adv Mater*. 1999;11:707–724.
- [51] Takezoe H, Takanishi Y. Bent-core liquid crystals: their mysterious and attractive world. *Jpn J Appl Phys*. 2006;45:597–625.
- [52] Takezoe H, Eremin A. Bent-shaped Liquid Crystals. Structures and Physical Properties. Boca Raton: CRC Press; 2017.
- [53] Tschierske C, Photinos DJ. Biaxial nematic phases. *J Mater Chem*. 2010;20:4263–4294.
- [54] Tschierske C, Zäschke H. A mild and convenient esterification of sensitive carboxylic acids. *J prakt Chem*. 1989;331:365–366.
- [55] Shanker G, Nagaraj M, Kocot A, et al. Nematic phases in 1,2,4-oxadiazole-based bent-core liquid crystals: is there a ferroelectric switching? *Adv Funct Mater*. 2012;22:1671–1683.
- [56] Vita F, Adamo FC, Francescangeli O. Polar order in bent-core nematics: an overview. *J Mol Liq*. 2018;267:564–573.
- [57] Vita F, Adamo FC, Pisani M, et al. Nanostructure of unconventional liquid crystals investigated by synchrotron radiation. *Nanomaterials*. 2020;10:1679.
- [58] Jakli A. Liquid crystals of the twenty-first century – nematic phase of bent-core molecules. *Liq Cryst Rev*. 2013;1:65–82.
- [59] de Vries A. X-ray photographic studies of liquid crystals I. A cybotactic nematic phase. *Mol Cryst Liq Cryst*. 1970;10:219–236.
- [60] Hong SH, Verduzco R, Williams JC, et al. Short-range smectic order in bent-core nematic liquid crystals. *Soft Matter*. 2010;6:4819–4827.
- [61] Ghilardi M, Adamo FC, Vita F, et al. Comparative 2H NMR and X-ray diffraction investigation of a bent-core liquid crystal showing a nematic phase. *Crystals*. 2020;10:284.
- [62] Shanker G, Prehm M, Nagaraj M, et al. 1,2,4-oxadiazole-based bent-core liquid crystals with cybotactic nematic phases. *ChemPhysChem*. 2014;15:1323–1335.
- [63] Francescangeli O, Vita F, Samulski ET. The cybotactic nematic phase of bent-core mesogens: state of the art and future developments. *Soft Matter*. 2014;10:7685–7691.

- [64] Gleeson HF, Kaur S, Görtz V, et al. The nematic phases of bent-core liquid crystals. *ChemPhysChem*. 2014;15:1251–1260.
- [65] Jang Y, Panov VP, Kocot A, et al. Short-range correlations seen in the nematic phase of bent-core liquid crystals by dielectric and electro-optic studies. *Phys Rev E*. 2011;84:060701(R).
- [66] Panarin YP, Sreenilayam SP, Vij JK, et al. Formation and development of nanometer-sized cybotactic clusters in bent-core nematic liquid crystalline compounds. *Beilstein J Nanotechnol*. 2018;9:1288–1296.
- [67] Vaupotic N, Szydłowska J, Salamoneczyk M, et al. Structure studies of the nematic phase formed by bent-core molecules. *Phys Rev E*. 2009;80:030701.
- [68] Zhang C, Gao M, Diorio N, et al. Direct observation of smectic layers in thermotropic liquid crystals. *Phys Rev Lett*. 2012;109:107802.
- [69] Gao M, Kim Y-K, Zhang C, et al. Direct observation of liquid crystals using cryo-TEM: specimen preparation and low-dose imaging. *Mic Res Technol*. 2014;77:754–772.
- [70] Chakraborty A, Das MK, Das B, et al. Rotational viscosity measurements of bent-core nematogens. *Soft Matter*. 2013;9:4273–4283.
- [71] Balachandran R, Panov VP, Vij JK, et al. Effect of cybotactic clusters on the elastic and flexoelectric properties of bent-core liquid crystals belonging to the same homologous series. *Phys Rev E*. 2013;88:032503.
- [72] Sreenilayam SP, Panarin YP, Vij JK, et al. Flexoelectric polarization studies in bent-core nematic liquid crystals. *Phys Rev E*. 2015;92:022502.
- [73] Madhuri PL, Hiremath US, Yelamagad CV, et al. Influence of virtual surfaces on Frank elastic constants in a polymer-stabilized bent-core nematic liquid crystal. *Phys Rev E*. 2016;93:042706.
- [74] Cestari M, Frezza E, Ferrarini A, et al. Crucial role of molecular curvature for the bend elastic and flexoelectric properties of liquid crystals: mesogenic dimers as a case study. *J Mater Chem*. 2011;21:12303–12308.
- [75] Varshini GV, Rao DSS, Hiremath US, et al. Dielectric and viscoelastic investigations in a binary system of soft- and rigid-bent mesogens exhibiting the twist-Bend nematic phase. *J Mol Liq*. 2012;323:114987.
- [76] Tadapatri P, Hiremath US, Yelamagad CV, et al. Patterned electroconvective states in a bent-core nematic liquid crystal. *J Phys Chem B*. 2010;114:10–21.
- [77] Krishnamurthy KS, Tadapatri P, Viswanatha P. Dislocations and metastable chevrons in the electroconvective in plane normal roll state of a bent core nematic liquid crystal. *Soft Matter*. 2014;10:7316–7327.
- [78] Jang Y, Panov VP, Keith C, et al. Sign reversal in the dielectric anisotropy as functions of temperature and frequency in the nematic phase of a bent-core liquid crystal. *Appl Phys Lett*. 2010;97:152903.
- [79] Tschierske C, Ungar G. Mirror symmetry breaking by chirality synchronisation in liquids and liquid crystals of achiral molecules. *ChemPhysChem*. 2016;17:9–26.
- [80] Tschierske C. Mirror symmetry breaking in liquids and liquid crystals. *Liq Cryst*. 2018;45:2221–2252.
- [81] Latinwo F, Stillinger FH, DeBenedetti G. Molecular model for chirality phenomena. *J Chem Phys*. 2016;145:154503.
- [82] Shanker G, Nagaraj M, Kocot A, et al. Nematic phases in 1,2,4-oxadiazole-based bent-core liquid crystals: is there a ferroelectric switching? *Adv Funct Mater*. 2012;22:1671–1683.
- [83] Goodby JW, Collings PJ, Kato, et al. *Handbook of Liquid Crystals*. 2nd ed. Vol. 5 (Weinheim: Wiley-VCH) 2014 ; p. 34–36.
- [84] Breckon R, Chakraborty S, Zhang C, et al. Nanostructures of nematic materials of laterally branched molecules. *ChemPhysChem*. 2014;15:1457–1462.
- [85] Kim Y-K, Cukrov G, Vita F, et al. Search for microscopic and macroscopic biaxiality in the cybotactic nematic phase of new oxadiazole bent-core mesogens. *Phys Rev E*. 2016;93:062701.
- [86] Kim Y-K, Majumdar M, Senyuk BI, et al. Search for biaxiality in a shape-persistent bent-core nematic liquid crystal. *Soft Matter*. 2012;8:8880–8890.
- [87] Nagaraj M, Panarin YP, Manna U, et al. Electric field induced biaxiality and the electrooptic effecting a bent-core nematic liquid crystal. *Appl Phys Lett*. 2010;96:011106.
- [88] Jang Y, Panov VP, Kocot A, et al. Optical confirmation of biaxial nematic (Nb) phase in a bent-core mesogen. *Appl Phys Lett*. 2009;95:183304.
- [89] Chiappini M, Drwenski T, van Roij R, et al. Biaxial, twist-bend, and splay-bend nematic phases of banana-shaped particles, revealed by lifting the “smectic blanket”. *Phys Rev Lett*. 2019;123:068001.
- [90] Ocak H, Bilgin-Eran B, Prehm M, et al. Effects of chain branching and chirality on liquid crystalline phases of bent-core molecules: blue phases, de Vries transitions and switching of diastereomeric states. *Soft Matter*. 2011;7:8266–8280.
- [91] Green AAS, Tuchband MR, Shao R, et al. Chiral incommensurate helical phase in a smectic of achiral bent-core mesogens. *Phys Rev Lett*. 2019;122:107801.
- [92] Lehmann A, Alaasar M, Poppe M, et al. Stereochemical rules govern the soft self-assembly of achiral compounds: understanding the heliconical liquid-crystalline phases of bent-core mesogens. *Chem Eur J*. 2020;26:4714–4733.
- [93] Nagaraj M, Lehmann A, Prehm M, et al. Evidence of a polar cybotactic smectic A phase in a new fluorine substituted bent-core compound. *J Mater Chem*. 2011;21:17098–17103.
- [94] Kim Y-K, Cukrov G, Xiang J, et al. Domain walls and anchoring transitions mimicking nematic biaxiality in the oxadiazole bent-core liquid crystal C7. *Soft Matter*. 2015;11:3963–3970.
- [95] Arakawa Y, Ishida Y, Komatsu K, et al. Thioether-linked benzylideneaniline-based twist-Bend nematic liquid crystal dimers: insights into spacer lengths, mesogenic arm structures, and linkage types. *Tetrahedron*. 2021;95:132351.
- [96] Cao Y, Feng C, Jakli A, et al. Deciphering chiral structures in soft materials via resonant soft and tender X-ray scattering. *Giant*. 2020;2:100018.

- [97] Lewandowski W, Vaupotič N, Pocięcha D, et al. Chirality of liquid crystals formed from achiral molecules revealed by resonant X-ray scattering. *Adv Mater.* **2020**;1905591.
- [98] Alaasar M, Prehm M, Nagaraj M, et al. A liquid crystalline phase with uniform tilt, local polar order and capability of symmetry breaking. *Adv Mater.* **2013**;25:2186–2191.
- [99] Alaasar M, Prehm M, May K, et al. 4-cyanoresorcinol-based bent-core mesogens with azobenzene wings: emergence of sterically stabilized polar order in liquid crystalline phases. *Adv Funct Mater.* **2014**;24:1703–1717.
- [100] Alaasar M, Prehm M, Poppe S, et al. Development of polar order by liquid-crystal self-assembly of weakly bent molecules. *Chem Eur J.* **2017**;23:5541–5556.
- [101] Alaasar M, Prehm M, Tamba M-G, et al. Development of polar order in the liquid crystalline phases of a 4-cyanoresorcinol-based bent-core mesogen with fluorinated azobenzene wings. *ChemPhysChem.* **2016**;17:278–287.
- [102] Alaasar M, Prehm M, Belau S, et al. Polar order, mirror symmetry breaking, and photoswitching of chirality and polarity in functional bent-core mesogens. *Chem Eur J.* **2019**;25:6362–6377.
- [103] Poppe M, Alaasar M, Lehmann A, et al. Controlling the formation of heliconical smectic phases by molecular design of achiral bent-core molecules. *J Mater Chem C.* **2020**;8:3316–3336.
- [104] Pocięcha D, Cepić M, Gorecka E, et al. Ferroelectric mesophase with randomized interlayer structure. *Phys Rev Lett.* **2003**;91:185501.
- [105] Shimbo Y, Gorecka E, Pocięcha D, et al. Electric-field-induced polar biaxial order in a nontilted smectic phase of an asymmetric bent-core liquid crystal. *Phys Rev Lett.* **2006**;97:113901.
- [106] Gupta M, Datta S, Radhika S, et al. Randomly polarised smectic A phase exhibited by bent-core molecules: experimental and theoretical studies. *Soft Matter.* **2011**;7:4735–4741.
- [107] Gomola K, Guo L, Pocięcha D, et al. An optically uniaxial antiferroelectric smectic phase in asymmetrical bent-core compounds containing a 3-aminophenol central unit. *J Mater Chem.* **2010**;20:7944–7952.
- [108] Sebastian N, Belau S, Eremin A, et al. Emergence of polar order and tilt in terephthalate based bent-core liquid crystals. *Phys Chem Chem Phys.* **2017**;19:5895–5905.
- [109] Shanker G, Prehm M, Nagaraj M, et al. Development of polar order in a bent-core liquid crystal with a new sequence of two orthogonal smectic and an adjacent nematic phase. *J Mater Chem.* **2012**;21:18711–18714.
- [110] Alaasar M, Prehm M, Poppe M, et al. Development of polar order and tilt in lamellar liquid crystalline phases of a bent-core mesogen. *Soft Matter.* **2014**;10:5003–5016.
- [111] Chakraborty S, Das MK, Keith C, et al. Study of ferro- and anti-ferroelectric polar order in mesophases exhibited by bent-core mesogens. *Mater Adv.* **2020**;1:5902.
- [112] Link DR, Natale G, Shao R, et al. Spontaneous formation of macroscopic chiral domains in a fluid smectic phase of achiral molecules. *Science.* **1997**;278:1924–1927.
- [113] Keith C, Prehm M, Panarin YP, et al. Development of polar order in liquid crystalline phases of a banana compound with a unique sequence of three orthogonal phases. *Chem Commun.* **2010**;46:3702–3704.
- [114] Sreenilayam S, Panarin YP, Vij JK, et al. Biaxial order parameter in the homologous series of orthogonal bent-core smectic liquid crystals. *Phys Rev E.* **2013**;88:012504.
- [115] Sreenilayam S, Panarin YP, Vij JK, et al. Physical properties of SmAb phase in an achiral bent-core smectic liquid crystals. *Ferroelectrics.* **2012**;431:196–201.
- [116] Sreenilayam S, Panarin YP, Vij JK, et al. Occurrence of five different orthogonal smectic phases in a bent-core (BC) liquid crystal. *Mol Cryst Liq Cryst.* **2015**;610:116–121.
- [117] Nagaraj M, Sreenilayam S, Panarin YP, et al. Electric field induced transformations and dielectric properties in non-tilted phases of a bent-core smectic liquid crystal. *Mol Cryst Liq Cryst.* **2011**;540:82–87.
- [118] Sreenilayam S, Nagaraj M, Panarin YP, et al. Properties of non-tilted bent-core smectic liquid crystals. *Mol Cryst Liq Cryst.* **2012**;553:140–146.
- [119] Sreenilayam S, Nagaraj M, Panarin YP, et al. Structure and polymorphism of biaxial bent-core smectic liquid crystals. *Mol Cryst Liq Cryst.* **2012**;553:133–139.
- [120] Sreenilayam S, Panarin YP, Vij JK, et al. Biaxial order parameter in an achiral bent-core smectic liquid crystals. *Ferroelectrics.* **2012**;431:190–195.
- [121] Wirth I, Diele S, Eremin A, et al. New variants of polymorphism in banana-shaped mesogens with cyano-substituted central core. *J Mater Chem.* **2001**;11:1642–1650.
- [122] Panarin YP, Nagaraj M, Vij JK, et al. Field-induced transformations in the biaxial order of non-tilted phases in a bent-core smectic liquid crystal. *Eur Phys Lett.* **2010**;92:26002.
- [123] Sreenilayam SP, Panarin YP, Vij JK, et al. Fast linear electrooptic effect in non-chiral bent core nematic liquid crystals. *Ferroelectrics.* **2016**;495:35–42.
- [124] Nagaraj M, Panarin YP, Vij JK, et al. Liquid crystal display modes in a nontilted bent-core biaxial smectic liquid crystal. *Appl Phys Lett.* **2010**;97:213505.
- [125] Sreenilayam SP, Panarin YP, Vij KJ, et al. Development of ferroelectricity in the smectic phases of 4-cyanoresorcinol derived achiral bent-core liquid crystals with long terminal alkyl chains. *Phys Rev Mater.* **2017**;1:035604.
- [126] Panarin YP, Sreenilayam SP, Swaminathan V, et al. Observation of an anomalous SmA-SmC-SmA phase sequence in a bent-core liquid crystal derived from 4-cyanoresorcinol. *Phys Rev Res.* **2020**;2:013118.
- [127] Sreenilayam SP, Panarin YP, Vij JK, et al. Spontaneous helix formation in non-chiral bent-core liquid crystals with fast linear electro-optic effect. *Nat Commun.* **2016**;7:11369.
- [128] Vij JK, Panarin YP, Sreenilayam SP, et al. Investigation of the heliconical smectic SmCSPFhel phase in achiral bent-core mesogens derived from 4-cyanoresorcinol. *Phys Rev Mater.* **2019**;3:045603.

- [129] Panarin YP, Nagaraj M, Sreenilayam S, et al. Sequence of four orthogonal smectic phases in an achiral bent-core liquid crystal: evidence for the SmAPa phase. *Phys Rev Lett.* **2011**;107:247801.
- [130] Lagerwall ST. *Ferroelectric and Antiferroelectric Liquid Crystals*. Weinheim: Wiley-VCH; **1999**.
- [131] Fukuda A, Takanishi Y, Isozaki T, et al. Antiferroelectric chiral smectic liquid crystals. *J Mater Chem.* **1994**;4:997–1016.
- [132] Takezoe H, Gorecka E, Cepic M. Antiferroelectric liquid crystals: interplay of simplicity and complexity. *Rev Mod Phys.* **2010**;82:897–937.
- [133] Nakata M, Shao R-F, MacLennan JE, et al. Electric-field-induced chirality flipping in smectic liquid crystals: the role of anisotropic viscosity. *Phys Rev Lett* **2006** . 96 ():067802
- [134] Panarin YP, Sreenilayam SP, Vij JK, et al. A fast linear electro-optical effect in a non-chiral bent-core liquid crystal. *J Mater Chem C.* **2017**;5:12585–12590.
- [135] Meyer C, Davidson P, Constantin D. Fredericksz-like transition in a biaxial smectic-A phase. *Phys Rev X.* **2021**;11:031012.
- [136] Mach P, Pindak R, Levelut A-M, et al. Structures of chiral smectic-C mesophases revealed by polarization-analyzed resonant x-ray scattering. *Phys Rev E.* **1999**;60:6793–6802.
- [137] Lagerwall JPF. Demonstration of the antiferroelectric aspect of the helical superstructures in Sm-C*, Sm-Ca*, and Sm-Ca* liquid crystals. *Phys Rev E.* **2005**;71:051703.
- [138] Panov VP, Shtykov NM, Fukuda A, et al. Self-assembled uniaxial and biaxial multilayer structures in chiral smectic liquid crystals frustrated between ferro- and antiferroelectricity. *Phys Rev E.* **2004**;69:060701(R).
- [139] Lazar C, Yang K, Glaser MA, et al. Ferroelectric liquid crystal induced by a bridged biphenyl dopant with helical topography. *J Mater Chem.* **2002**;12:586–592.
- [140] Greco C, Ferrarini A. Entropy-driven chiral order in a system of achiral bent particles. *Phys Rev Lett.* **2015**;115:147801.
- [141] Matsuyama A. Phase transitions of heliconical smectic-C and heliconical nematic phases in banana-shaped liquid crystals. *Phys Rev E.* **2020**;101:050701(R).
- [142] Abberley JP, Killah R, Walker R, et al. Heliconical smectic phases formed by achiral molecules. *Nat Commun.* **2018**;9:228.
- [143] Salamończyk M, Vaupotič N, Pocięcha D, et al. Multi-level chirality in liquid crystals formed by achiral molecules. *Nat Commun.* **2019**;10:1922.
- [144] Mandle RJ, Goodby JW. A twist-Bend nematic to an intercalated, anticlinic, biaxial phase transition in liquid crystal bimesogens. *Soft Matter.* **2016**;12:1436–1443.
- [145] Walker R, Pocięcha D, Storey JMD, et al. Remarkable smectic phase behaviour in odd-membered liquid crystal dimers: the CT6O.m series. *J Mater Chem C.* **2021**;9:5167–5173.
- [146] Beguin L, Emsley JW, Lelli M, et al. The chirality of a twist-Bend nematic phase identified by NMR spectroscopy. *J Phys Chem B.* **2012**;116:7940–7951.
- [147] Ivšić T, Vinković M, Baumeister U, et al. Milestone in the NTB phase investigation and beyond: direct insight into molecular self-assembly. *Soft Matter.* **2014**;10:9334–9342.
- [148] Stevenson WD, Zeng XB, Welsch C, et al. Macroscopic chirality of twist-Bend nematic phase in bent dimers confirmed by circular dichroism. *J Mater Chem C.* **2020**;8:1041–1047.
- [149] Salamończyk M, Mandle RJ, Makal A, et al. Double helical structure of the twist-Bend nematic phase investigated by resonant X-ray scattering at the carbon and sulfur K-edges. *Soft Matter.* **2018**;14:9760–9763.
- [150] Stevenson WD, Ahmed Z, Zeng XB, et al. Molecular organization in the twist-Bend nematic phase by resonant X-ray scattering at the Se K-edge and by SAXS, WAXS and GIXRD. *Phys Chem Chem Phys.* **2017**;19:13449–13454.
- [151] Emsley JW, Lelli M, Lesage A, et al. A comparison of the conformational distributions of the achiral symmetric liquid crystal dimer CB7CB in the achiral nematic and chiral twist-bend nematic phases. *J Phys Chem B.* **2013**;117:6547–6557.
- [152] Shi Y, Sun Z, Chen R, et al. Effect of conformational chirality on optical activity observed in a smectic of achiral, bent-core molecules. *J Phys Chem B.* **2017**;121:6944–6950.
- [153] Matsuyama A. Twist-bend nematic phases of banana-shaped molecules with an axial chirality. *Liq Cryst.* **2019**;46:2301–2321.
- [154] Toxvaerd S. Molecular dynamics simulations of isomerization kinetics in condensed fluids. *Phys Rev Lett.* **2000**;22:4747–4750.
- [155] Dressel C, Reppe T, Prehm M, et al. Chiral self-sorting and amplification in isotropic liquids of achiral molecules. *Nat Chem.* **2014**;6:971–977.
- [156] Zeng X, Ungar G. Spontaneously chiral cubic liquid crystal: three interpenetrating networks with twist. *J Mater Chem.* **2020**;8:5389–5398.
- [157] Lu H, Zeng XB, Ungar G, et al. The solution of the puzzle of smectic-Q: the phase structure and the origin of spontaneous chirality. *Angew Chem Int Ed.* **2018**;57:2835–2840.
- [158] Dressel C, Liu F, Prehm M, et al. Dynamic mirror-symmetry breaking in bicontinuous cubic phases. *Angew Chem Int Ed.* **2014**;53:13115–13120.
- [159] Reppe T, Poppe S, Cai X, et al. Spontaneous mirror symmetry breaking in benzil-based soft crystalline, cubic liquid crystalline and isotropic liquid phases. *Chem Sci.* **2020**;11:5902–5908.
- [160] Zeldovich YB. Pseudoscalar liquid crystals. *Zh Eksp Teor Fiz.* **1971**;67:2357–2361.
- [161] Kats EI. Spontaneous chiral symmetry breaking in liquid crystals. *Low Temp Phys.* **2017**;43:5–7.
- [162] Takezoe H. Spontaneous achiral symmetry breaking in liquid crystalline phases. *Top Curr Chem.* **2012**;318:303–330.
- [163] Jacques J, Collet A, Wilen SH. *Enantiomers, racemates, and resolutions*. New York: J. Wiley & Sons, Inc; **1981**.
- [164] Dutta S, Gellman AJ. Enantiomer surface chemistry: conglomerate versus racemate formation on surfaces. *Chem Soc Rev.* **2017**;46:7787–7839.

- [165] Fuhrhop J-H, Helfrich W. Fluid and solid fibers made of lipid molecular bilayers. *Chem Rev.* **1993**;93:1585.
- [166] Novotna V, Glogarova M, Kaspar M, et al. Reentrant orthogonal smectic-A phase below a tilted smectic-C phase in a chiral compound. *Phys Rev E.* **2011**;83:020701(R).
- [167] Weissflog W, Lischka C, Diele S, et al. The inverse phase sequence SmA–SmC in symmetric dimeric liquid crystals. *Liq Cryst.* **2000**;27:43–50.
- [168] Mertelj A, Cmok L, Sebastián N, et al. Splay nematic phase. *Phys Rev X.* **2018**;8:041025.
- [169] Chen X, Körblova E, Dong D, et al. First-principles experimental demonstration of ferroelectricity in a thermotropic nematic liquid crystal: polar domains and striking electro-optics. *Proc Natl Acad Sci USA.* **2020**;117:14021–14031.
- [170] Chiappini M, Dijkstra M. A generalized density-modulated twist-splay-Bend phase of banana-shaped particles. *Nat Commun.* **2021**;12:2157.
- [171] Revignas D, Ferrarini A. From bend to splay dominated elasticity in nematics. *Crystals.* **2021**;11:831.
- [172] Fernández-Rico C, Chiappini M, Yanagishima T, et al. Shaping colloidal bananas to reveal biaxial, splay-Bend nematic, and smectic phases. *Science.* **2020**;369:950–955.
- [173] Pelzl G, Eremin A, Diele S, et al. Spontaneous chiral ordering in the nematic phase of an achiral banana-shaped compound. *J Mater Chem.* **2002**;12:2591–2593.
- [174] Görtz V, Southern C, Roberts NW, et al. Unusual properties of a bent-core liquid-crystalline fluid. *Soft Matter.* **2009**;5:463–471.
- [175] Salter PS, Tschierske C, Elston SJ, et al. Flexoelectric measurements of a bent-core nematic liquid crystal. *Phys Rev E.* **2011**;84:031708.
- [176] Jang Y, Balachandran R, Keith C, et al. Chirality of an achiral bent-core nematic mesogens observed in planar and homeotropic cells under certain conditions. *Soft Matter.* **2012**;8:10479–10485.
- [177] Dietrich CF. Lyotropic nematic liquid crystals: interplay between small twist elastic constant and chirality effects under confined geometries. *Liq Cryst Today.* **2021**;30:2–14.
- [178] Longa L, Pająk G, Wydro T. Chiral symmetry breaking in bent-core liquid crystals. *Phys Rev E.* **2009**;7:040701(R).
- [179] Pleiner H, Brand HR. Tetrahedral order in liquid crystals. *Braz J Phys.* **2016**;46:565–595.
- [180] Hough LE, Spannuth M, Nakata M, et al. Chiral isotropic liquids from achiral molecules. *Science.* **2009**;325:452–456.
- [181] Le KV, Takezoe H, Araoka F. Chiral superstructure mesophases of achiral bent-shaped molecules – hierarchical chirality amplification and physical properties. *Adv Mater.* **2017**;1602737.
- [182] Westphal E, Gallardo H, Sebastian N, et al. Liquid crystalline self-assembly of 2,5-diphenyl-1,3,4-oxadiazole based bent-core molecules and the influence of carbosilane end-groups. *J Mater Chem.* **2019**;7:3064–3081.
- [183] Yoshizawa A. Molecular design of flexible liquid crystal oligomers stabilising the chiral frustrated phases. *Liq Cryst.* **2017**;44:1877–1893.
- [184] Westphal E, Gallardo H, Caramori GF, et al. Polar order and symmetry breaking at the boundary between bent-core and rodlike molecular forms. When 4-cyanoresorcinol meets carbosilane end groups. *Chem Eur J.* **2016**;22:8181–8197.
- [185] Alaasar M, Prehm M, Tschierske C. Influence of halogen substituent on the mesomorphic properties of five-ring banana-shaped molecules with azobenzene wings. *Liq Cryst.* **2013**;40:656–668.
- [186] Alaasar M, Prehm M, Tschierske C. A new room temperature dark conglomerate mesophase formed by bent-core molecules combining 4-iodoresorcinol with azobenzene units. *Chem Commun.* **2013**;49:11062–11064.
- [187] Alaasar M, Prehm M, Brautzsch M, et al. 4-methylresorcinol-based bent-core liquid crystals with azobenzene wings – a new class of compounds with dark conglomerate phases. *J Mater Chem C.* **2014**;2:5487–5501.
- [188] Alaasar M, Prehm M, Brautzsch M, et al. Dark conglomerate phases of azobenzene derived bent-core mesogens – relationships between the molecular structure and mirror symmetry breaking in soft matter. *Soft Matter.* **2014**;10:7285–7296.
- [189] Alaasar M, Prehm M, Tschierske C. Helical nano-crystallite (HNC) phases: chirality synchronization of achiral bent-core mesogens in a new type of dark conglomerates. *Chem Eur J.* **2016**;22:6583–6597.
- [190] Alaasar M, Prehm M, Tschierske C. Mirror symmetry breaking in fluorinated bent-core mesogens. *RSC Adv.* **2016**;6:82890–82899.
- [191] Keith C, Reddy RA, Prehm M, et al. Layer frustration, polar order and chirality in liquid crystalline phases silyl-terminated achiral bent-core molecules. *Chem Eur J.* **2007**;13:2556–2577.
- [192] Lansac Y, Maiti PK, Clark NA, et al. Phase behavior of bent-core molecules. *Phys Rev E.* **2003**;67:011703.
- [193] Chattham N, Tamba M-G, Stannarius R, et al. Leaning-type polar smectic-C phase in a freely suspended bent-core liquid crystal film. *Phys Rev E.* **2015**;91:030502(R).
- [194] Chattham N, Korblova E, Shao R, et al. de Gennes' triclinic smectics – not so far-fetched after all. *Liq Cryst.* **2009**;36:1309–1317.
- [195] Kovářová A, Světlík S, Kozmík V, et al. Unusual polymorphism in new bent-shaped liquid crystals based on biphenyl as a central molecular core. *Beilstein J Org Chem.* **2014**;10:794–807.
- [196] Chen W-H, Chuang W-T, Jeng U-S, et al. New SmCG phases in a hydrogen-bonded bent-core liquid crystal featuring a branched siloxane terminal group. *J Am Chem Soc.* **2011**;133:15674–15685.
- [197] Zhang C, Diorio N, Radhika S, et al. Two distinct modulated layer structures of an asymmetric bent-shape smectic liquid crystal. *Liq Cryst.* **2012**;39:1149–1153.

- [198] Ocak H, Poppe M, Bilgin-Eran B, et al. Effects of molecular chirality on self-assembly and switching in liquid crystals at the cross-over between rod-like and bent shapes. *Soft Matter*. 2016;12:7405–7422.
- [199] Walba DM, Körblova E, Shao R, et al. A ferroelectric liquid crystal conglomerate composed of racemic molecules. *Science*. 2000;288:2181–2184.
- [200] Kumazawa K, Nakata M, Araoka F, et al. Important role played by interlayer steric interactions for the emergence of the ferroelectric phase in bent-core mesogens. *J Mater Chem*. 2004;14:157–164.
- [201] Zhang Y, O’Callaghan MJ, Baumeister U, et al. Bent-core mesogens with branched carbosilane termini: flipping suprastructural chirality without reversing polarity. *Angew Chem Int Ed*. 2008;47:6892–6896.
- [202] Ocak H, Bilgin Eran B, Nuray S, et al. Extraordinary magnetic field effects on the LC phases of homochiral and racemic 4-cyanoresorcinol-based diamagnetic bent-core mesogens. *J Mater Chem C*. 2021;9:1895–1910.
- [203] Domenici V, Marini A, Veracini CA, et al. Effect of the magnetic field on the supramolecular structure of chiral smectic C phases: 2HNMR studies. *ChemPhysChem*. 2007;8:2575–2587.
- [204] Domenici V, Veracini CA, Novotna V, et al. Twist grain boundary liquid-crystalline phases under the effect of the magnetic field: a complete 2H and 13C NMR study. *ChemPhysChem*. 2008;9:556–566.
- [205] Ocak H, Canli NY, Bilgin Eran B. synthesis, mesomorphic and dielectric properties of new bent-core liquid crystal with a terminal lactate group. *J Mol Struct*. 2021;1223:128975.
- [206] Le KV, Hafuri M, Ocak H, et al. Unusual electro-optic Kerr response in a self-stabilized amorphous blue phase with nanoscale smectic clusters. *ChemPhysChem*. 2016;17:1425–1429.
- [207] Gim M-J, Hur S-T, Park KW, et al. Photoisomerization-induced stable liquid crystalline cubic blue phase. *Chem Commun*. 2012;48:9968–9970.
- [208] Gim M-J, Han G, Choi SW, et al. Thermal phase transition behaviours of the blue phase of bent-core nematogen and chiral dopant mixtures under different boundary conditions. *Soft Matter*. 2014;10:8224–8228.
- [209] Liu H, Shen D, Wang X, et al. Wide blue phase range induced by bent-shaped molecules with acrylate end groups. *Opt Mater Exp*. 2016;6:436.
- [210] Ocak H, Bilgin-Eran B, Güzeller D, et al. Twist grain boundary (TGB) states of chiral liquid crystalline bent-core mesogens. *Chem Commun*. 2015;51:7512–7515.
- [211] Reddy RA, Sadashiva BK, Baumeister U. Liquid crystalline properties of unsymmetrical bent-core compounds containing chiral moieties. *J Mater Chem*. 2005;15:3303–3316.
- [212] Taushanoff S, Van Le K, Williams J, et al. Stable amorphous blue phase of bent-core nematic liquid crystals doped with a chiral material. *J Mater Chem*. 2010;20:5893–5898.
- [213] Alaasar M, Poppe S, Kerzig C, et al. Cluster phases of 4-cyanoresorcinol derived hockey-stick liquid crystals. *J Mater Chem C*. 2017;5:8454–8468.
- [214] Kosata B, Tamba G-M, Baumeister U, et al. Liquid-crystalline dimers composed of bent-core mesogenic units. *Chem Mater*. 2006;18:691–701.
- [215] Wang Y, Yoon HG, Bisoyi HK, et al. Hybrid rod-like and bent-core liquid crystal dimers exhibiting biaxial smectic a and nematic phases. *J Mater Chem*. 2012;22:20363–20367.
- [216] Shanker G, Prehm M, Tschierske C. Laterally connected bent-core dimers and bent-core-rod couples with nematic liquid crystalline phases. *J Mater Chem*. 2012;22:168–174.
- [217] Yelamaggad CV, Prasad SK, Nair GG, et al. Low-molar-mass, monodisperse, bent-rod dimer exhibiting biaxial nematic and smectic a phases. *Angew Chem Int Ed*. 2004;43:3429–3432.
- [218] Wang Y, Zheng Z-G, Bisoyi HK, et al. Thermally reversible full color selective reflection in a self-organized helical superstructure enabled by a bent-core oligomesogen exhibiting a twist-Bend nematic phase. *Mater Horiz*. 2016;3:442–446.